Ball Grid Array-Module With Integrated Shaped Lens for WiGig Applications in Eyewear Devices

Aimeric Bisognin, *Student Member, IEEE*, Aykut Cihangir, Cyril Luxey, *Senior Member, IEEE*, Gilles Jacquemod, *Member, IEEE*, Romain Pilard, *Member, IEEE*, Frédéric Gianesello, *Member, IEEE*, Jorge R. Costa, *Senior Member, IEEE*, Carlos A. Fernandes, *Senior Member, IEEE*, Eduardo B. Lima, *Student Member, IEEE*, Chinthana J. Panagamuwa, *Member, IEEE*, and William G. Whittow, *Senior Member, IEEE*

***Abstract*—A ball grid array-module (BGA-module) incorporating a low-cost shaped dielectric lens is proposed for wireless communications in the 60-GHz WiGig band between a smart eyewear, where it is integrated and facing a laptop or TV. The module, which is codesigned with a 60-GHz transceiver, consists of two separate identical antennas for transmitting (Tx) and receiving (Rx). The in-plane separation of these elements is 6.9 mm both being offset from the lens focus. This poses a challenge to the lens design to ensure coincident beam pointing directions for Rx and Tx. The shaped lens is further required to narrow the angular coverage in the elevation plane and broaden it in the horizontal plane. A 3-D-printed eyewear frame with an integrated lens and a recess for proper BGA-module integration is fabricated in ABS-plastic material. Measurements show a reflection coefficient below −12 dB in the 57–66 GHz band. A maximum gain of 11 dBi is obtained at 60 GHz, with 24° and 96° beamwidth at 5-dBi gain, respectively, in the vertical and horizontal planes. The radiation exposure is evaluated for a homogeneous SAM head phantom and a heterogeneous visible human head. The simulated power density values for both models are found to be lower than the existing standards.**

***Index Terms*—60 GHz, antenna-in-package, eyewear, lens antennas, plastic packaging, WiGig.**

I. Introduction

WITH the never-ending improvement of the capabilities of wireless communication devices, the most critical necessity has been to supply the user with higher and higher data rates. This has led to both the improvement of the existing wireless communication standards as well as the launch of new standards and new technologies. One of these standards, the WiGig IEEE 802.11ad, is gaining more and more popularity among industries because the unlicensed frequency band around 60 GHz offers a broad bandwidth to achieve multigigabits speeds (up to 7 Gbit/s). The low interference level favored by the very high wall penetration loss and by the high oxygen absorption in this band for moderate distances makes this standard a good candidate for line-of-sight (LoS) in-room wireless personal area communications (WPAN). Possible applications include the wireless connection of a personal computer (PC) with its peripheral devices (monitor, keyboard, etc.), as well as ultra-high-definition video/audio transfer from a camera to a TV or projector, eliminating the need for cables. Typically, for a LoS 2-meter communication in this band, an antenna gain of approximately 4 dBi is needed (at both sides of the link) considering today's transceiver performances (10 dBm power at the antenna port, -54 dBm Rx sensitivity and OFDM 16-QAM modulation). If this distance is increased to around 8 m, the gain should be approximately 10 dBi.

In parallel, smart eyewear devices are gaining popularity as wireless communicating objects with some products already released in the market and some other being prepared for the near future [1]–[5]. In general, those devices incorporate a small optical lens-reflector screen, a camera, a microphone/speaker pair, and a touchpad. They are generally connected to a peripheral (smartphone or set-top box) through Bluetooth or WLAN standards at 2.4 GHz. Our recent work considered eyewear devices as a possible candidate to replace smartphones in the near future and we successfully demonstrated high potential for LTE communications [6].

In this study, a ball grid array-module (BGA-module) incorporating separate Tx and Rx antennas (to avoid a lossy switch at 60 GHz in TDD mode) integrated with a shaped 3-D-printed plastic lens is proposed for integration with a smart eyewear device for high-speed video transfer from the device to a laptop or a TV in front of the user. The transceiver is based on an RFIC design using 65 nm CMOS technology and aims to fulfill the WiGig requirements for its highest available data rate, i.e., MCS20. This mode offers a 4.158-Gbps data rate thanks to OFDM 16-QAM modulation. All WiGig frequency subbands are covered from 57 to 66 GHz. The chipset is described in detail in [7]. The shaped lens is intended to achieve an acceptable gain (> 10 dBi) and to shape the radiation pattern

Manuscript received November 16, 2014; revised November 05, 2015; accepted December 19, 2015. Date of publication XXXX XX, XXXX; date of current version XXXX XX, XXXX.

A. Bisognin is with EpOC, Université Nice Sophia Antipolis, Valbonne, France, and also with STMicroelectronics, Crolles, France.

A. Cihangir and G. Jacquemod are with EpOC, Université Nice Sophia Antipolis, Valbonne, France.

C. Luxey is with EpOC, Université Nice Sophia Antipolis, Valbonne, France, and also with Institut Universitaire de France (IUF), Paris, France (e-mail: cyril.luxey@unice.fr).

R. Pilard and F. Gianesello are with STMicroelectronics, Crolles, France.

C. Fernandes and E. Lima are with Instituto de Telecomunicações, Instituto Superior Técnico, University of Lisbon, Lisbon, Portugal.

J. Costa is with DCTI, Instituto Universitário de Lisboa (ISCTE-IUL), and Instituto de Telecomunicações, Lisbon, Portugal.

C. Panagamuwa and W. Whittow are with the Wireless Communications Research Group, School of Electronic, Electrical and Systems Engineering, Loughborough University, Loughborough, LE11 3TU, U.K. (e-mail: w.g.whittow@lboro.ac.uk, C.J.Panagamuwa@lboro.ac.uk).

Color versions of one or more of the figures in this paper are available online at http://ieeexplore.ieee.org.

Digital Object Identifier 10.1109/TAP.2016.2517667

with wide beamwidth in the horizontal plane (at least 100° at 5 dBi gain) and narrow beamwidth in the vertical plane (in the order of 25° at 5 dBi gain). The challenge for its design is the additional need to counteract the beam depointing effect due to the impossibility of positioning the separate Tx and Rx radiating elements simultaneously at the lens single focal point. The in-plane separation of these radiating elements is 6.9 mm. The lens was found to be a convenient solution to address the shaped beam challenge instead of using a large planar array with low aperture efficiency and nonuniform (and lossy) feeding network. The objective of the paper is to show that the proposed antenna concept is feasible for mm-wave eyewear applications, being compact, low cost and with negligible impact in terms of head specific absorption rate (SAR). Section II gives some basic information about the BGA-module and the Tx and Rx radiating elements. The design of the lens with its theoretical background and simulation results are also explained in this section. The integration of the BGA-module and the lens within the eyewear is presented in Section III. Simulation results taking into account the presence of the user's head are also presented in this section. Measurement results for the manufactured prototype are given in Section IV. Section V discusses the evaluation of the radiation exposure on the body through simulations. Finally, conclusion is drawn in Section VI.

II. Antenna Design

A. BGA-Module

The BGA-module was designed and manufactured in high density integration (HDI) technology dedicated to 60 GHz SiP solutions. This HDI technology is based on standard BGA design and realization techniques: it enables a minimum trace resolution as well as trace spacing of 50 µm. The low-cost stack-up of three organic substrates enables four metallization layers. A picture of the BGA-module can be seen in Fig. 1. This module was designed to radiate in free-space. The module has equal length and width (12×12 mm^2) with a height of 0.5 mm. It hosts two printed antennas, one for receiving and one for transmitting, offset from the center of the BGA-module and separated by $\Delta d = 6.9$ mm distance from each other ($1.38\ \lambda_0$). The antennas are of aperture-coupled patch type, where the apertures are excited through a microstrip line underneath them. The antennas are linearly polarized with a measured gain higher than 4 dBi between 57 and 66 GHz (including transmission line losses). More information about the BGA-module (version 1) and the antenna can be found in [8]. They are thus not repeated here for the sake of brevity. However, it should be noted that a second optimized version of the BGA-module is used in the current paper having more than 10 dB return loss and 5 dBi gain from 57 to 66 GHz which is better than the performance presented in [8].

B. Lens Design

A small shaped lens is used directly on top of the patch elements of BGA-module to modify its radiation pattern into a more convenient shape for the intended application. The gain is required to exceed 5 dBi within a 100° angular interval in the horizontal plane (H-plane, or yz-plane in Fig. 2) and 25° angular interval in the vertical plane (E-plane or xz-plane in Fig. 2). This gives the user enough margin to look comfortably at the screen from different angles without compromising the data link. It should be noted that no codesign between the source and the lens was achieved as we reused the existing BGA-module version 2 dedicated to radiate in free space (and not plastic medium).

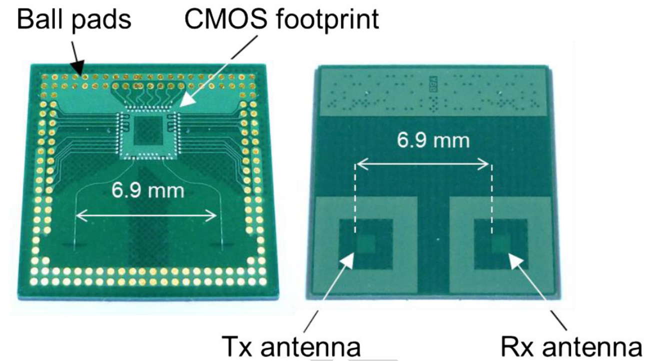

Fig. 1. Picture of the BGA-module version 2: bottom view on left and top view on right.

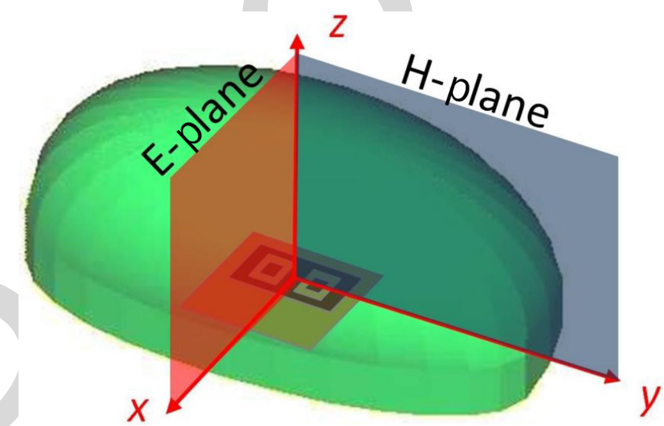

Fig. 2. Schematic view of the optimized 3-D-lens placed above the BGA-module with axis definition.

The radiation pattern described in the paragraph above is not symmetric and therefore requires a full 3-D shaped lens. Although geometrical optics (GO) formulations exist for the design of arbitrary shaped dielectric lenses subject to arbitrarily output power template conditions [9]–[10], it is shown in this study that for the present radiation pattern specifications it is enough to consider a far simpler and computationally fast alternative based on a modification of the GO formulation for axial symmetric lenses.

The combination with physical optics (PO) analysis enables faster optimization of the shape of the 3-D lens compared to the exact 3-D GO formulation, offering a very reasonable agreement with the targeted radiation pattern beamwidths.

The GO/PO-based lens design procedure requires prior knowledge of the radiation pattern of one antenna of the BGA-module into an unbound medium of the chosen material for

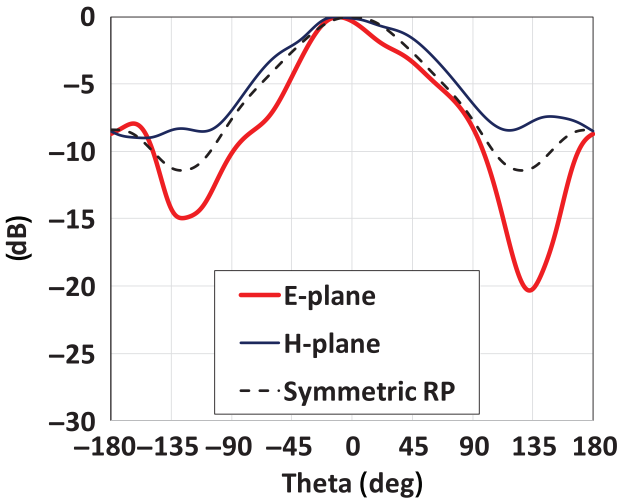

Fig. 3. Normalized simulated E- and H-plane radiation patterns of the BGA-module (Tx-antenna) in an unbounded medium of ABS plastic. Symmetric RP is an average of the E- and H-planes further used for the lens design.

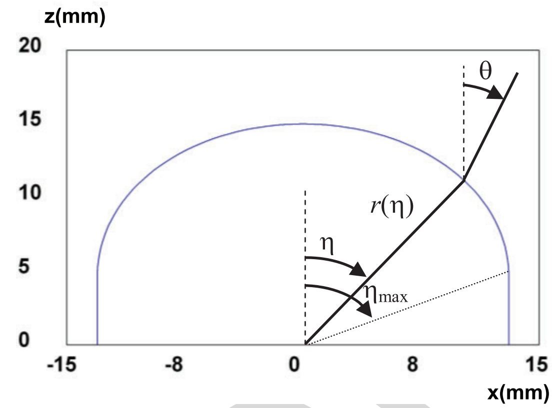

Fig. 4. Horizontal (or H-plane) profile of the plastic lens.

the lens. ABS-M30 plastic material (consumer grade plastic used for smartphone casing) was chosen in order to ensure low cost for the overall system. A 3-D-printing rapid manufacturing technology was selected to fabricate the lens. A disk sample of ABS material was printed to experimentally evaluate its complex permittivity. The Fabry–Perot resonator measurement method presented in [11] gave us $\epsilon_r = 2.48$ and $\tan(\delta) = 0.009$ at 60 GHz. The lens design was performed at 60 GHz, as the central frequency. Intrinsic to the GO design, the frequency bandwidth of the lens is inherently large but the full-system bandwidth is mainly determined by the BGA-module bandwidth. The radiation pattern of the feed inside the unbounded ABS medium at 60 GHz was obtained from a full-wave HFSS simulation (Fig. 3). Overall, the main E- and H-planes of the bare BGA antennas have similar beamwidths. The 3-D shaped lens is designed in two steps. First, the lens profile in the horizontal plane is obtained from an elevation cut of an axial-symmetric lens designed with an appropriate GO formulation. Then, the design rule for the lens profile in the vertical plane is defined and the complete 3-D lens physical shape is obtained from an adequate combination of both horizontal and vertical lens profiles.

Fig. 4 shows the general geometry for the lens design procedure. The axial symmetric lens profile is represented by $r(\eta)$ where $r(\eta = 0°) = 15$ mm corresponds to the total height of the lens. The feed, corresponding to one patch of the BGA-module, is assumed initially to be at the center of the base of the lens and in direct contact with it. The lens design assumes that the feed is positioned at the center of the lens. However, the target radiation pattern $G(\theta)$ that is needed to define the lens shape is carefully optimized to minimize its dependence with feed offset when the BGA-module is integrated at the base of the lens. At this point, the lens design formulation requires that the feed radiation pattern $U(\eta)$ is axial symmetric. The symmetric $U(\eta)$ power pattern is generated as an average of the cocomponents in the main planes of the BGA antenna (symmetric RP curve in Fig. 3). The obtained $U(\eta)$ function is represented in Fig. 3 by the black dashed curve (symmetric RP). Other symmetrization options could have been adopted for the feed radiation pattern. They would imply different $r(\eta = 0)$ values and different $G(\theta)$ shape from what we obtained in the optimization process. The selected target pattern $G(\theta)$ is a flat-top type with a sharp drop-off at $\theta = 60°$ to comply with the desired full 100° beamwidth in the horizontal plane of the lens.

The lens profile $r(\eta)$ is designed to transform $U(\eta)$ into a target axial symmetric power pattern $G(\theta)$. The $r(\eta)$ profile is obtained by solving a set of two differential equations defined by the authors in [12]. The integration is performed for increasing η angles up to the $\eta_{\max}$ value where $\partial r(\eta)/\partial\eta$ becomes negative. This $\eta_{\max}$ angle defines the edge of the lens (Fig. 4). The remaining points in the lens profile from $z = r(\eta_{\max})\ \cos(\eta_{\max})$ to $z = 0$ are defined with a constant value of $x = r(\eta_{\max})\ \sin(\eta_{\max})$. By forcing nonnegative $\partial r(\eta)/\partial\eta$, the lens surface will not diffract the radiation of the feed into the negative z direction, i.e., into the user. The analytical formulation is valid for arbitrary initial values $r(\eta = 0°)$ which acts as a scaling factor. In the axial symmetric lens, the matching between the output power pattern and the horizontal plane target improves as $r(\eta = 0°)$ increases. This value influences the vertical plane power pattern in a different way, as will be discussed ahead. In the present design, $r(\eta = 0°) = 15$ mm was chosen as a compromise between the output power pattern specification in both planes and the utmost size constraint for the desired integration with the glasses. The obtained lens profile is presented in Fig. 4. This curve is used as the horizontal profile of the 3-D lens. In the vertical plane (E-plane), narrowing the radiation pattern of the BGA-module can be achieved by using a beam collimating lens profile (like an ellipse). For each cut of the 3-D lens at a constant x value, an elliptical lens profile is implemented (Fig. 5). Each x-cut corresponds to a given η angle so that $x = r(\eta)\sin(\eta)$. In each x-cut, the height of the elliptical profile is $F(\eta) = r(\eta)\cos(\eta)$. The elliptical lens profile is defined by

$$l\left(\eta,\alpha\right) = \frac{\sqrt{\varepsilon_r} - 1}{\sqrt{\varepsilon_r} - \cos\left(\alpha\right)} F\left(\eta\right) \quad (1)$$

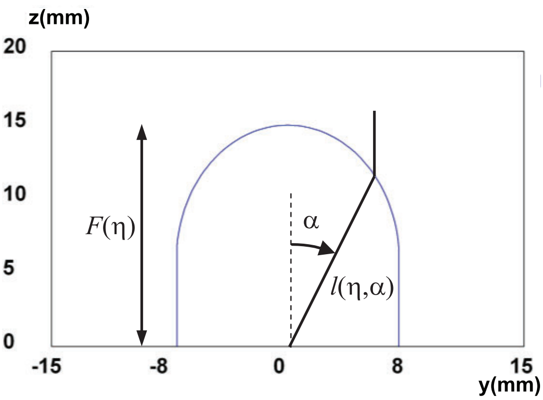

Fig. 5. Vertical cut of the plastic lens profile for a x = constant plane.

where α is the angle of each point $l(\eta, \alpha)$ in relation to the vertical axis of each cut plane of the lens profile as indicated in Fig. 5. Therefore, the complete 3-D lens profile is defined by the following set of parametric equations

$$\begin{aligned} x(\eta, \alpha) &= r(\eta) \sin(\eta) \\ y(\eta, \alpha) &= l(\eta, \alpha) \sin(\alpha) \\ z(\eta, \alpha) &= l(\eta, \alpha) \cos(\alpha). \end{aligned} \tag{2}$$

As with η, the α angle also ranges from 0 to $\alpha_{\max}$ where $\partial l(\eta\alpha)/\partial\alpha$ becomes negative. The remaining points from $z = z(\eta, \alpha_{\max})$ to $z = 0$ are defined with a constant $y = y(\eta, \alpha_{\max})$.

The obtained 3-D lens profile is shown in Fig. 2. Its overall size is $\Delta z = 15$ mm by $\Delta x = 26$ mm and $\Delta y = 14$ mm. This approximate 3-D lens design procedure is an evolution of the one developed by the authors in [13]. The corresponding radiation pattern is calculated using PO, considering the actual nonsymmetric feed radiation pattern shown in Fig. 3.

The normalized result is presented in Fig. 6(a) for the main planes, confirming the effectiveness of the proposed design. The simulated maximum directivity is of the order of 12 dBi. To achieve a narrower E-plane radiation pattern and a higher lens directivity, the lens size can be increased by choosing a higher value for $r(\eta = 0°)$.

Due to the Rx and Tx $\Delta d = 6.9$ mm separation in the BGA-module, the lens is not fed from its focal point at the center of the base of the lens. The $\Delta d/2 = 3.45$ mm (0.69 λ_0 at 60 GHz) feed off-set in the x-axis tends to produce a beam depointing effect. However, the previous H-plane radiation pattern template was specifically chosen to minimize this effect. It is noted that the y-plane elliptical profile does not allow depointing minimization if y-axis feed off-set was selected instead. The x-axis feed off-set effect in the horizontal plane (H-plane) radiation pattern of the lens can be seen in Fig. 6(b), showing that the flat-top characteristic is reasonably maintained and only 1 dB reduction is observed in the broadside direction from the nonoffset source case. It has little influence in the E-plane since Tx and Rx patches remain in the focal point of the elliptical x-cut profile of the lens that passes through each feed position.

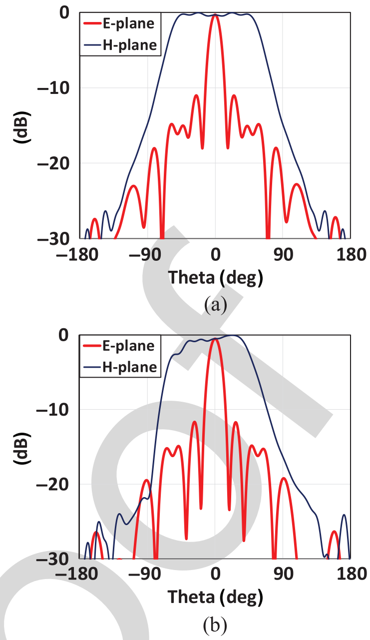

Fig. 6. Normalized GO/PO simulated radiation pattern of the 3-D lens fed by the Tx patch of the BGA-module at 60 GHz. (a) Feed at the center of the lens. (b) Feed offset from the center by x = 3.45 mm.

III. Integration of the BGA-Module With the Eyewear Device

In order to validate the GO/PO-based lens design and to evaluate the antenna in the realistic use-case scenario, full wave electromagnetic simulations were also carried out, using the commercial software Empire XCcel [14]. The simulation model included the BGA-module integrated with the dielectric lens, mounted in the left-hand side of a dedicated ABS eyewear frame (Fig. 7 left part). An FR4 substrate which might be needed in a realistic product as the application PCB and a backing ground plane was also included in this model, behind the antenna-module (Fig. 8). The frame includes a curved region on the right-hand side of the head to emulate visually the screen of a smart eyewear device. It also includes on the two sides of the frame, two parallelepiped casing-like structures for housing the application PCBs for WLAN/Bluetooth and WiGig standards, respectively.

A homogeneous specific anthropomorphic mannequin (SAM) head was also included in the simulation to account for the user head influence. Considering the computation time and memory requirements to simulate the full set-up from Fig. 7, it was decided to use a cropped model of the head, since the effects of the tissues that are placed far from the antenna in terms of wavelength will be negligible. The cropped model used in the simulations can be seen in Fig. 7 (right side). It keeps all the structures and materials that lie within 10 λ_0 distance from the Antenna-module and discards all the others, so the final dimensions of the simulation rectangular box is $78 \times 73 \times 155$ mm^3. The lens and the dielectric frame were modeled as ABS plastic material. The values taken from Fabry–Perot measurements and given in Section II B were used to

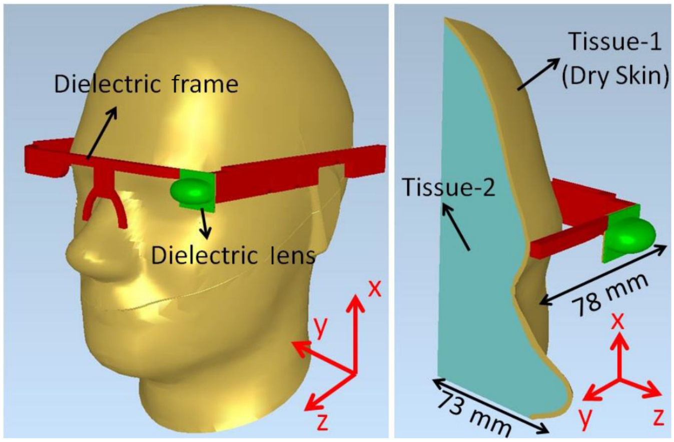

Fig. 7. Simulation model of the BGA-module integrated with the lens and the ABS eyewear frame close to the SAM Head. The shaped lens is on the frame left side.

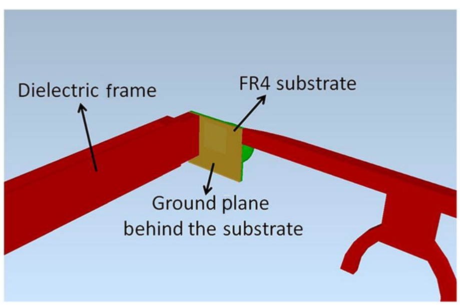

Fig. 8. Position of the FR4 substrate and the ground plane which is backing the antenna-module.

model the ABS material. The outer shell of the head (marked as Tissue-1) was assigned the properties of dry skin at 60 GHz, having a relative permittivity of 7.98 and a loss tangent of 1.37. To model the interior region of the head (Tissue-2), electrical properties of the brain was used, with a relative permittivity of 10.4 and loss tangent of 1.19. Those values were taken from [15].

A second set of simulations was also performed removing the head and the backing PCB of the lens. The comparison of the simulated reflection coefficient of the Tx antenna of the BGA-module with the lens without the head and PCB and with the head and PCB is presented in Fig. 9. The simulated coupling coefficient from the Tx antenna to Rx antenna is very low ($|S_{21}| < -30$ dB) and thus is not shown here. The Tx antenna integrated with the lens with the backing PCB and head has a reflection coefficient always lower than -6.7 dB between 57 and 66 GHz, even decreasing below -15 dB around the lower edge of the band. It can also be seen from the same figure that the reflection coefficient of the same Tx antenna without backing PCB and head is very similar, suggesting negligible effects of the head and the backing PCB. The consequence of the absence of a codesign between the source and the lens directly translates into a frequency shift (compared to the "without head and PCB case") with a minimum of $|S_{11}|$ around 55–57 GHz (almost out-of-band) as the BGA-module now radiates into plastic rather than air.

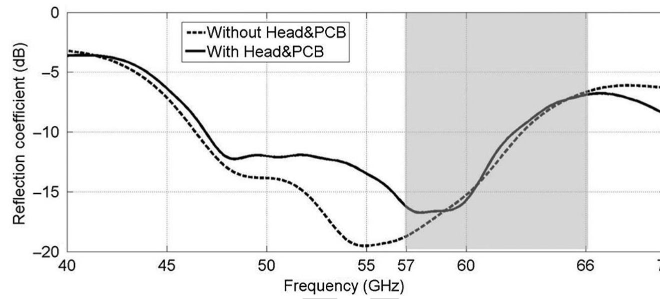

Fig. 9. Simulated reflection coefficient for the Tx patch of the BGA-module integrated with the lens without the Head and PCB and with the Head and PCB.

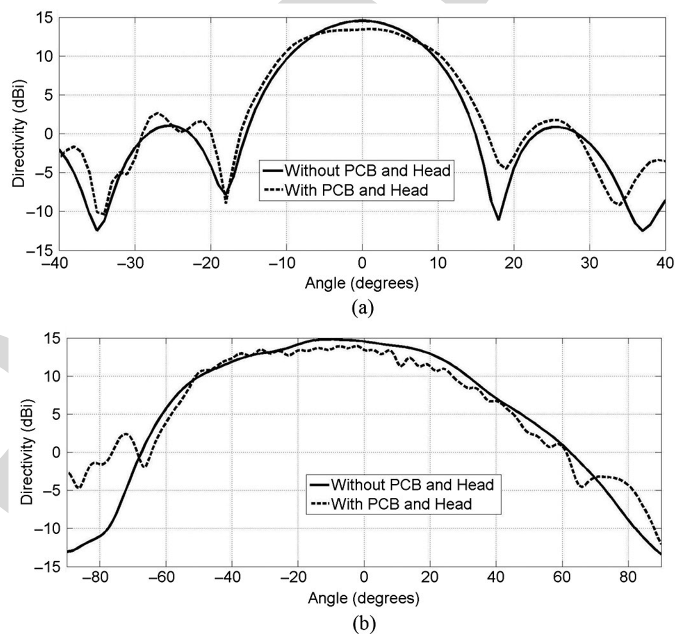

Fig. 10. Full-wave simulated directivity patterns of the BGA-module integrated with the lens with head and PCB and without head and PCB. (a) E-plane and (b) H-plane at 60 GHz.

The comparison of the full-wave radiation patterns in the E-plane ($\varphi = 0°$) and H-plane ($\varphi = 90°$) for the two configurations is shown in Fig. 10(a) and (b), respectively. The maximum radiation does not occur exactly in the front direction of the eyewear. There is a slight asymmetry in the radiation pattern (10° tilt) but this is not really important in this application as the beam tilt is small as compared to the beamwidth and the user does not necessarily have to be directly in front of the receiving device. Note that the obtained radiation patterns confirm that the lens geometry is fairly suitable to overcome the focal depointing. In addition, the specified 5 dBi gain beamwidth of 25° in the E-plane and 100° in the H-plane is very closely met. The maximum full-wave simulated directivity is almost 15 dBi which is higher than the 12 dBi simulated with GO/PO. We anticipate that the difference is mainly the result of known limitations of the GO/PO asymptotic method for small-size lenses. Also, it is known that a surface wave may appear for elliptical lenses at the lens/air interface which, for some lens sizes, can lead to higher directivity than predicted with GO/PO [16]. The head and the PCB behind the antenna-module have little

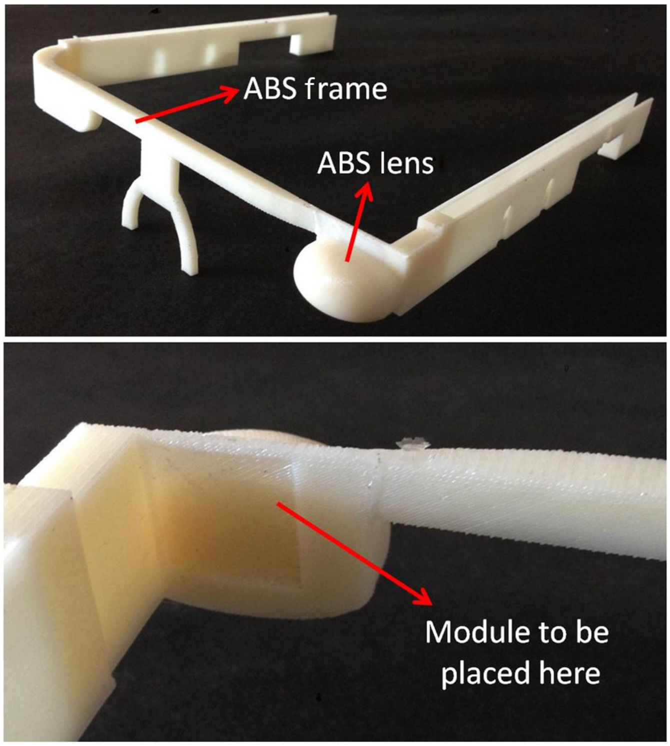

Fig. 11. Pictures of the manufactured ABS frame incorporating the shape of the lens.

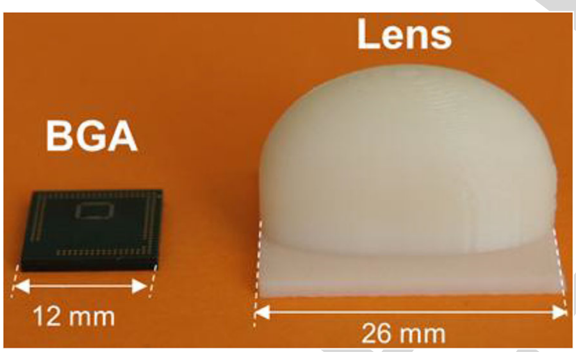

Fig. 12. BGA-module and 3-D-printed ABS plastic lens.

effects (but not significant) in the general radiation pattern (1 dB reduction of the directivity and broader beam is the E-plane); however, we decided to omit this last configuration in the next simulation studies and measurements.

IV. Measurements

A. Fabrication of the Eyewear Prototype and the Antenna-Module

A picture of the manufactured ABS frame integrating the lens is shown in Fig. 11. Fig. 12 presents the BGA-module (left side) and the ABS lens alone (right side). All the ABS prototypes were fabricated using 3-D printing plastic technology.

B. Measurement Results

The measurements of the BGA-module with the integrated lens were carried out without the head and PCB, following the

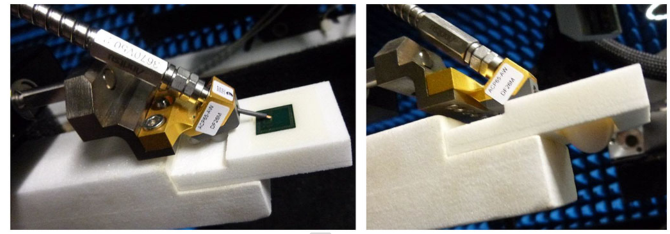

Fig. 13. Pictures of the probing of the Tx antenna of the BGA-module with the lens (left side), bottom view of the BGA-module with the lens inside the foam support (right side).

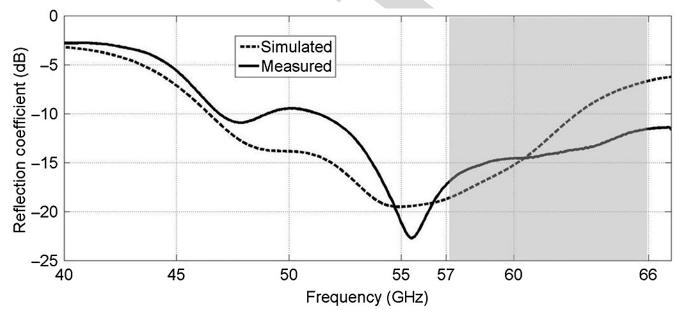

Fig. 14. Simulated and measured reflection coefficient of the Tx antenna of the BGA-module with the lens.

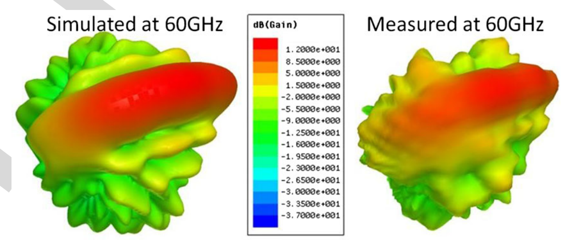

Fig. 15. Simulated and measured 3-D realized gain patterns of the BGA-module with the lens at 60 GHz.

conclusion from the previous section. Also, the full eyewear frame was not utilized for the radiation pattern measurements as it physically impairs the access of the feeding probe used in our millimeter-wave measurement set-up [17] (Fig. 13).

There is a good agreement between measured and simulated reflection coefficients given in Fig. 14. The measured reflection coefficient is well below -11.5 dB in the target band (57–66 GHz). Note, no codesign was performed which suggests that better performance could be achieved in a possible new version of the eyewear and BGA-module. The simulated and measured realized gain patterns are presented in 3-D form in Fig. 15 and in the main planes in Fig. 16(a) (E-plane for $\varphi = 0°$) and Fig. 16(b) (H-plane for $\varphi = 90°$). The maximum measured gain is approximately 11 dBi at 60 GHz (including the transmission line losses). The measured 5 dBi gain beamwidth is 24° in E-plane and 96° in H-plane. A comparison of the simulated and measured radiation efficiency can be seen in Fig. 17. A fair agreement is observed, especially in the target band between 57 and 66 GHz. The measured efficiency has been extracted from the 3-D realized gain pattern with the method already presented in [18]. The Tx antenna of the BGA-module has a measured radiation efficiency ranging from 52% to 58% in this band which is a suitable value for WiGig transmissions between

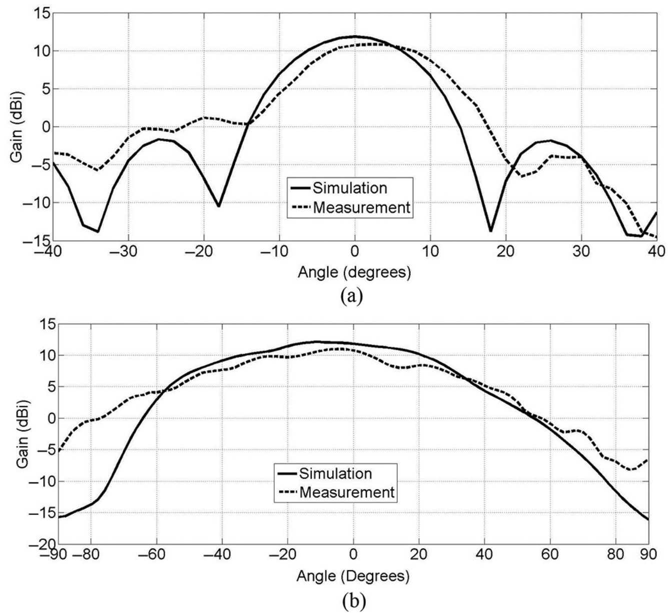

Fig. 16. Simulated and measured realized gain of the BGA-module with the lens in (a) E-plane and (b) H-plane at 60 GHz.

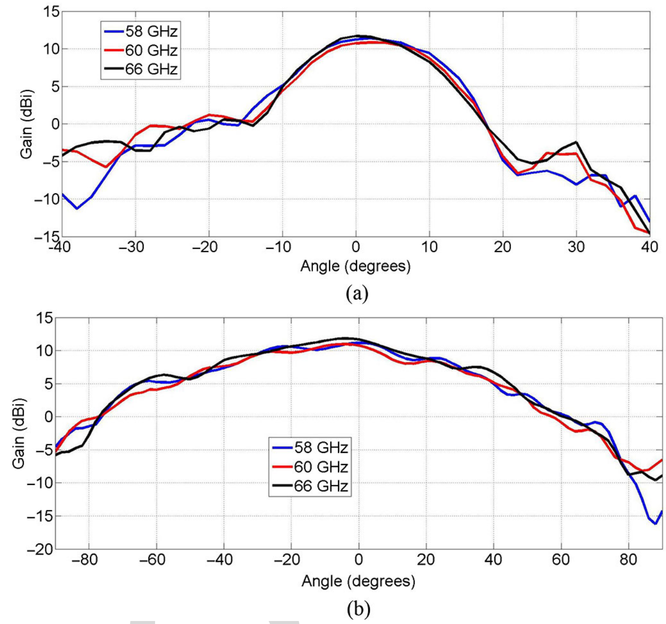

Fig. 18. Measured realized gain in (a) E-plane and (b) H-plane of the Tx antenna of BGA-module with the lens for different frequencies.

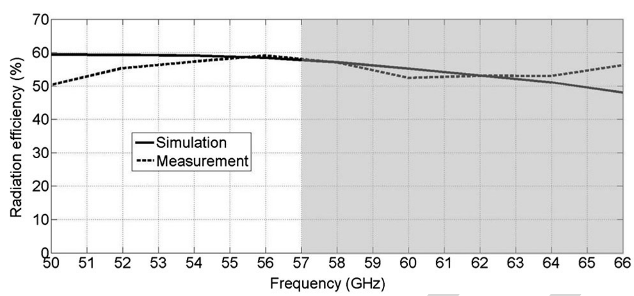

Fig. 17. Simulated and measured radiation efficiency of the Tx antenna from the BGA-module with the lens.

TABLE I
COMPARISON OF MEASURED BEAMWIDTH AT DIFFERENT FREQUENCIES

	58 GHz	60 GHz	66 GHz	Target
E-plane 5 dBi BW	25°	24°	23°	25°
H-plane 5 dBi BW	106°	96°	108°	100°

the eyewear and a TV or a laptop. The stability of the gain pattern versus frequency was also investigated through the band of interest. Fig. 18 presents the measured realized gain patterns (E- and H-planes) for three frequency points: 58, 60, and 66 GHz. These patterns show negligible variation with respect to frequency even in terms of 5 dBi beamwidth as presented in Table I, all complying with the beamwidth specification.

V. HUMAN BODY EXPOSURE

International standards based on the incident power density have been developed to limit the electromagnetic exposure by the human body from RF devices at 60 GHz. The IEEE (USA) recommends a maximum power density of $10\ \mathrm{W/m^2}$ averaged over $0.01\ \mathrm{m}^2 (10\ \mathrm{cm} \times 10\ \mathrm{cm})$ averaged over 3.6 min for the general public [19]. The limit is $100\ \mathrm{W/m^2}$ in controlled environments averaged over 21.6 s [19]. The standards also determine a maximum power density of $1000\ \mathrm{W/m^2}$ averaged over any one square centimeter. ICNIRP (Europe) has power density limits of, respectively, $10\ \mathrm{W/m^2}$ and $50\ \mathrm{W/m^2}$ averaged over $20\ \mathrm{cm^2}$ for the general public and controlled conditions. The maximum power density averaged over $1\ \mathrm{cm^2}$ should not exceed 20 times the above values. The averaging time can be calculated by $68/\mathrm{f}1.05 = 0.92$ min. The ICNIRP levels are stricter for both the larger averaging areas and also the $1\ \mathrm{cm^2}$ area. Therefore, compliance with ICNIRP guarantees compliance with the IEEE recommendation. Despite the power density being defined in the standards, there is no consistent evaluation metric in the recent published papers. The local specific absorption rate (SAR) is examined in [20] and [21]. The 1-g SAR and the power absorbed were discussed in [22]. The maximum electric field, power density, and local SAR were assessed in [23]. *In vitro* protein and culture were considered in [24] and [25] where the maximum local SAR and the SAR averaged over the whole sample was related to the incident power density. A thermal imaging camera was used to measure the temperature distribution and hence the local and average power density as well as the local SAR in [26]. This paper concluded that power levels up to 550 mW would comply with the exposure limit and an incident power density of $10\ \mathrm{W/m^2}$ would result in a temperature increase of 0.1°C.

In our study, two sets of simulations were performed for analyzing the effect of the BGA-module with lens on the head of the user. The first set of simulations was performed with a homogeneous head model as used in Section III, consisting of the outer part modeled as dry skin and the inner part modeled as the brain tissue. The second set of simulations was performed

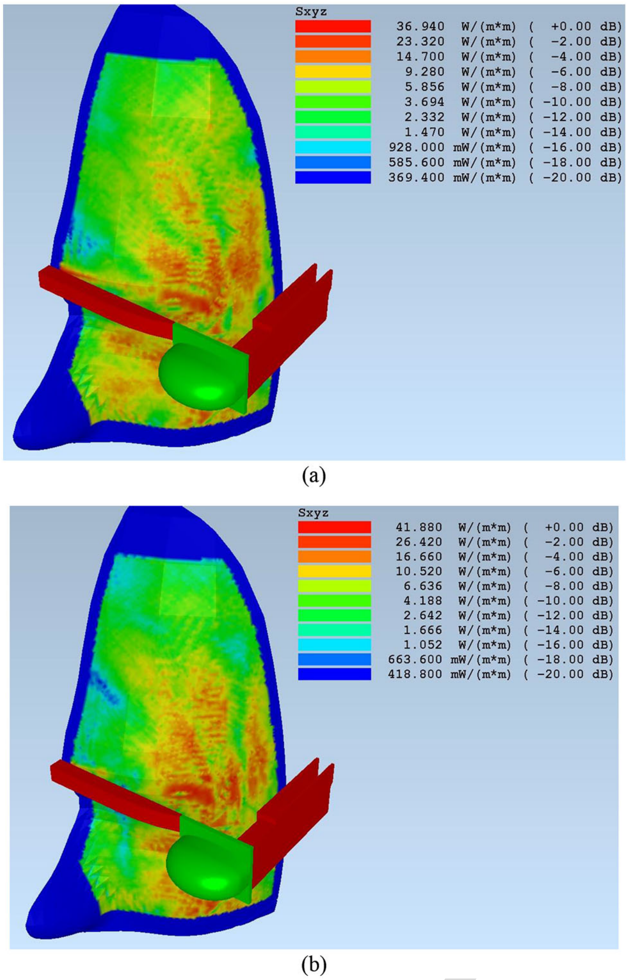

Fig. 19. Simulated power density with SAM head (scaled to 1 W input power) over the skin for (a) 60 GHz and (b) 66 GHz.

with the visible human head model taking into account different tissues with corresponding electrical properties.

A. Simulations With Homogeneous Head Model

Simulations with the homogeneous head model were performed to obtain the power density level at the surface of the skin. According to ICNIRP guidelines, the power density level on the tissue, averaged over 20 cm^2 should be lower than 1 mW/cm^2 (or 10 W/m^2) around 60 GHz frequency. The simulated power density with EMPIRE XCcel software on the skin surface can be observed in Fig. 19 for 60 and 66 GHz. It should be noted here that the values presented in this figure legends are not averaged either over time or space, so they are the worst-case levels. Moreover, the input power to the antenna was set as 1 W in the simulations so the power density levels shown in this figure need to be divided by 100 to comply with the typical input power level of 10 dBm for WiGig devices. The unaveraged maximum power density observed on the skin surface varies between 0.37 and 0.42 W/m^2 between 60–66 GHz (for an input power of 10 dBm). These values are well below the reference values from the guidelines even though they are instantaneous, unaveraged values. Obtaining such a low-power density over the skin was expected since the main radiation is directed away from the head and also the spacing between the antenna-module and the head is 30 mm which is 6 λ_0 at 60 GHz.

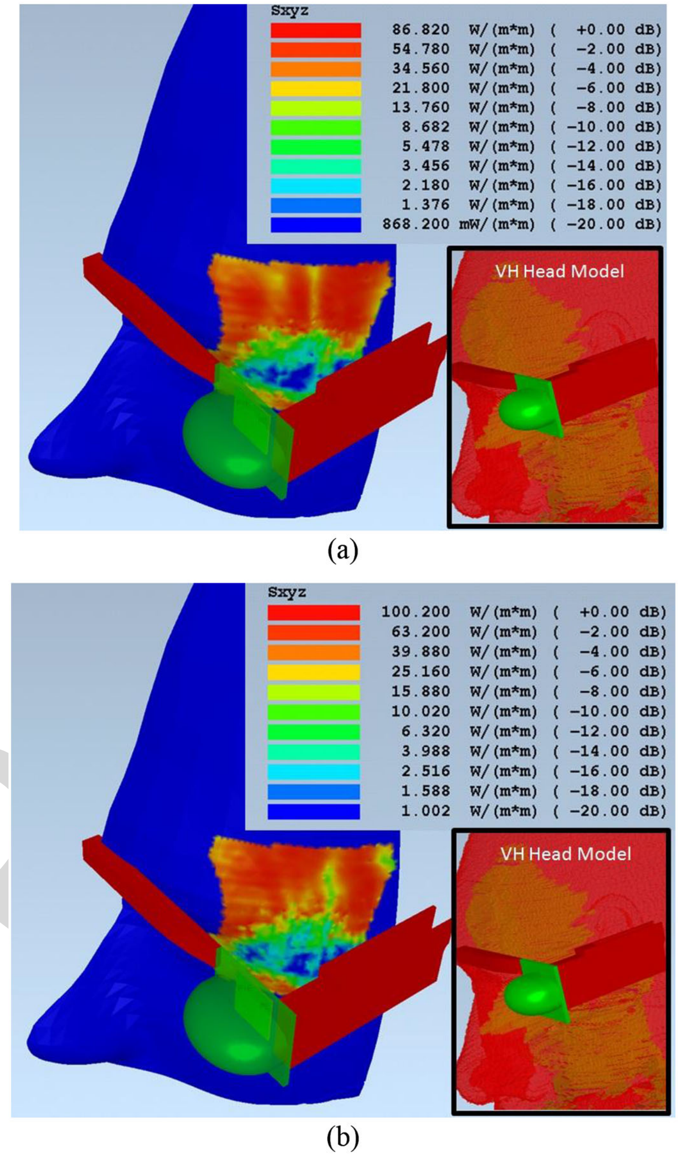

Fig. 20. Simulated power density with VH head (scaled to 1 W input power) for (a) 60 GHz and (b) 66 GHz.

B. Simulations With Visible Human Head Model

The simulations were also performed by placing the BGA-module with lens on a truncated VH model with 1 mm resolution (inset in Fig. 20). The Yee cell size inside the head was set to 0.2 mm and even smaller cells were used to discretize the BGA-module including the lens. Empire can display the power density on the surface of the SAM head, which is categorized as a solid shape, but not on the voxel-based VH head. Therefore, to examine the power density on the surface of the VH head, the SAM-shaped field monitor was copied to the VH simulation file. This allowed us to observe that the surface of the VH head was closer to the antenna than the SAM head. Therefore, the SAM-shaped field monitor was moved several millimeters toward the antenna to lie on the surface of the VH head. Approximate calculations using the path loss equation indicated that this positioning difference can increase the power density by approximately 5 dB. The power density on the surface of the VH head varies between 67 and 100 W/m^2 as shown in Fig. 20. These values are again the maximum values seen at a point in space, normalized to 1 W input power, without any space or time averaging. Considering 10nbsp;dBm of maximum input power in WiGig applications, the values are well below the standard values, even without averaging.

VI. Conclusion

This paper demonstrated the feasibility of a compact low-cost antenna assembly for a WiGig smart eyewear device intended for high-speed wireless data communication in the 60-GHz band with a laptop or TV facing the user. The antenna-module incorporates a 3-D-printed shaped dielectric lens especially designed to enhance gain while shaping the radiation pattern to provide wide angular coverage in the horizontal plane and narrow beam coverage in the vertical plane. The lens design was based on GO/PO but full wave electromagnetic simulation was carried out to evaluate the antenna assembly performance when integrated with the eyewear device. Results were presented for two scenarios: the first one included the user's head as well as a portion of a PCB backing the antenna-module. In the second scenario, the head and PCB were removed. It was demonstrated that the effect of the head and of the backing PCB on the radiation pattern and the reflection coefficient was negligible. Keeping this in mind, the measurements for the BGA antenna-module and the lens were carried out in free-space, showing a good agreement with the simulations in terms of reflection coefficient, radiation efficiency, and realized gain radiation pattern. The maximum measured gain at 60 GHz was 11 dBi, with 5 dBi gain beamwidth of 24° in the vertical plane and 96° in the horizontal plane (including the transmission line losses). The measured gain radiation pattern was also shown to have negligible variation over the target frequency band (57–66 GHz).

The effects of the antenna radiation on the human body was analyzed for two sets of simulations, using both a homogeneous SAM head phantom and visible human head model. The simulated power density values for both head models were found to be lower than the limits established in the related standards, considering an input power of 10 dBm.

Acknowledgment

The authors would like to acknowledge Orange Labs La Turbie and the CIM-PACA design platform. F. Devillers from Orange Labs is deeply acknowledged for the adjustments of the mechanical parts of the measurement set-up. They would also like to acknowledge a scholarship given by project ESF RNP "Newfocus" to Aimeric Bisognin.

References

[1] *Google Glass* [Online]. Available: http://www.google.com/glass/start/

[2] *M100 Smart Glass* [Online]. Available: http://www.vuzix.com/UKSITE/consumer/products_m100.html

[3] *RECON Jet* [Online]. Available: http://www.reconinstruments.com/products/jet/

[4] *Olympus MEG4.0* [Online]. Available: http://www.olympus.co.jp/jp/news/2012b/nr120705meg40j.jsp

[5] *Optinvent ORA* [Online]. Available: http://optinvent.com/see-through-glasses-ORA

[6] A. Cihangir *et al.*, "Feasibility study of 4G cellular antennas for eyewear communicating devices," *IEEE Antennas Wireless Propag. Lett.*, vol. 12, pp. 1704–1707, 2013.

[7] A. Siligaris *et al.*, "A 65 nm CMOS fully integrated transceiver module for 60 GHz wireless HD applications," *IEEE J. Solid-State Circuits*, vol. 46, no. 12, pp. 162–164, Dec. 2011.

[8] R. Pilard *et al.*, "HDI organic technology integrating built-in antennas dedicated to 60 GHz SiP solution," in *Proc. IEEE Antennas Propag. Soc. Int. Symp. (AP-SURSI)*, Chicago, IL, USA, Jul. 2012, pp. 8–14.

[9] C. Salema, C. A. Fernandes, and R. K. Jha, *Solid Dielectric Horn Antennas*. Norwood, MA, USA: Artech House, 1998.

[10] R. Sauleau and B. Bares, "A complete procedure for the design and optimization of arbitrarily shaped integrated lens antennas," *IEEE Trans. Antennas Propag.*, vol. 54, no. 4, pp. 1122–1133, Apr. 2006.

[11] C. A. Fernandes and J. R. Costa, "Permittivity measurement and anisotropy evaluation of dielectric materials at millimeter-waves," in *Proc. IMEKO World Congr.*, Lisboa, Portugal, Sep. 2009.

[12] C. A. Fernandes, "Shaped dielectric lenses for wireless millimeter-wave communications," *IEEE Antennas Propag. Mag.*, vol. 41, no. 5, pp. 141–150, Oct. 1999.

[13] C. A. Fernandes, "Design of shaped lenses for non-symmetric cells in MBS," in *Proc. IEEE Antennas Propag. Soc. Int. Symp. (AP-S/URSI)*, Orlando, FL, USA, Jul. 1999, vol. 3, pp. 2440–2443.

[14] *EMPIRE XCcel* [Online]. Available: http://www.empire.de/

[15] [Online]. Available: http://www.itis.ethz.ch/itis-for-health/tissue-properties/database/tissue-frequency-chart/

[16] D. Pasqualini and S. Maci, "High-frequency analysis of integrated dielectric lens antennas," *IEEE Trans. Antennas Propag.*, vol. 52, no. 3, pp. 840–847, Mar. 2004.

[17] D. Titz, F. Ferrero, and C. Luxey, "Development of a millimeter-wave measurement setup and dedicated techniques to characterize the matching and radiation performance of Probe-fed Antennas," *IEEE Antennas Propag. Mag.*, vol. 54, no. 4, pp. 188–203, Aug. 2012.

[18] D. Titz, F. Ferrero, P. Brachat, C. Luxey, and G. Jacquemod, "Efficiency measurement of probe-fed antennas operating at millimeter-wave frequencies," *IEEE Antennas Wireless Propag. Lett.*, vol. 11, pp. 1194–1197, Oct. 2012.

[19] *IEEE Standard for Safety Levels With Respect to Human Exposure to Radio Frequency Fields 3 kHz to 300 GHz*, IEEE Standard C95.1-2005, pp. 1–250, 2006.

[20] N. Chahat, C. Leduc, M. Zhadobov, and R. Sauleau, "Antennas and Interaction with the Body for Body Centric Wireless Communications at Millimeter Waves," in *Proc. Eur. Conf. Antennas Propag. (EuCAP)*, 2013, pp. 772–775.

[21] K. H. Chan, S. W. Leung, Y. L. Diao, Y. M. Siu, and K. T. Ng, "Analysis of millimeter wave radiation to human body using inhomogeneous multilayer skin model," in *Proc. Asia-Pac. Symp. Electromagn. Compat. (APEMC)*, 2012, pp. 721–724.

[22] A. R. Guraliuc, M. Zhadobov, G. Valerio, and R. Sauleau, "Enhancement of on-body propagation at 60 GHz using electro textiles," *IEEE Antennas Wireless Propag. Lett.*, vol. 13, pp. 603–606, Apr. 2014.

[23] M. Kouzai, A. Nishikata, T. Sakai, and S. Watanabe, "Characterization of 60 GHz millimeter-wave focusing beam for living-body exposure experiments," in *Proc. EMC'09*, 2009, pp. 309–312.

[24] M. Zhadobov *et al.*, "Evaluation of the potential biological effects of the 60-GHz millimeter waves upon human cells," *IEEE Trans. Antennas Propag.*, vol. 57, no. 10, pp. 2949–2956, Oct. 2009.

[25] M. Zhadobov, R. Sauleau, R. Augustine, C. Le Quément, Y. Le Dréan, and D. Thouroude, "Near-field dosimetry for in vitro exposure of human cells at 60 GHz," *Bioelectromagnetics*, vol. 33, no. 1, pp. 55–64, Jan. 2012.

[26] N. Chahat, M. Zhadobov, L. Le Coq, S. I. Alekseev, and R. Sauleau, "Characterization of the interactions between a 60-GHz antenna and the human body in an off-body scenario," *IEEE Trans. Antennas Propag.*, vol. 60, no. 12, pp. 5958–5965, Dec. 2012.

Q5 **Aimeric Bisognin** (S'xx) was born in Toulouse, France, in 1989. He received the Engineering degree in electronics from Polytech'Nice Sophia, Sophia Antipolis, France, in 2012, and the M.S. degree in telecommunications from EDSTIC, Sophia Antipolis, France, in 2012, and the Ph.D. degree in electronics engineering (with Hons.) from the University of Nice Sophia-Antipolis, France, in 2015.

During his Ph.D., he worked with the Electronique pour Objets Communicants (EpOC) Laboratory, STMicroelectronics, Crolles, France. He is currently a Postdoctoral Researcher with the EpOC Laboratory. He has authored or coauthored 8 publications in journals and 19 publications in international conferences. His research interests include millimeter-wave communications, especially in the field of the design and measurement of antenna in package, lens and reflector antennas for the 60, 80, and 120 GHz frequency bands.

Aykut Cihangir was born in Ankara, Turkey, in 1985. He received the Bachelor's degree in electrical Q6 and electronics engineering and the Master's degree from Middle East Technical University (METU), Ankara, Turkey, in 2010, and the Ph.D. degree from the University of Nice-Sophia Antipolis (UNSA), Nice, France, in 2007, 2010, and 2014, respectively.

Q7 From 2007 to 2011, he was with the Aerospace Industry as a Communication Systems Design Engineer in Unmanned Aerial Vehicle projects. Then, he was as a Postdoctoral Researcher with the EpOC team, UNSA. His research interests include electrically small antennas, matching networks, and mobile terminal antennas.

Cyril Luxey (SM'xx) was born in Nice, France, in 1971. He received the Master's degree (DEA) and the Ph.D. degree in electrical engineering (both with Hons.) from the University Nice-Sophia Antipolis, Nice, France, in 1996 and 1999, respectively.

During his thesis, he worked on printed leaky-wave antennas, quasi-optical mixers, and retrodirective transponders. From 2000 to 2002, he was with Alcatel, Mobile Phone Division, Colombes, France, where he was involved in the design and integration of internal antennas for commercial mobile phones. In 2003, he was an Associate Professor with the Polytechnic School, University Nice Sophia-Antipolis. Since 2009, he has been a Full Professor with the IUT Réseaux et Télécoms in Sophia-Antipolis, Valbonne, France. He is doing his research in the EpOC Laboratory as the Vice-Deputy of this laboratory. In October 2010, he was a Junior Member of the Institut Universitaire de France (IUF). Also, he collaborates with Berkeley Wireless Research Center, Berkeley, CA, USA, and Stanford University, Stanford, CA, USA, on mm-wave front-end transceivers at mm-wave frequencies. He also works on electrically small antennas, multiantenna systems for diversity, and MIMO techniques. He has authored or coauthored more than 250 papers in refereed journals, in international and national conferences and as book chapters. He has given more than 10 invited talks. His research interests include the design and measurement of millimeter-wave antennas, antennas-in-package, plastic lenses, and organic modules for 60, 120, and 240 GHz frequency bands.

Dr. Luxey is an Associate Editor for the IEEE ANTENNAS AND WIRELESS PROPAGATION LETTERS, a Regular Reviewer for several IEEE and IET journals and several European and US conferences in the field of microwave, microelectronics, and antennas. He has been the General Chair of the Loughborough Antennas and Propagation Conference 2011, the Award and Grant Chair of EuCAP 2012, and the Invited Paper CoChair of EuCAP 2013. He will be the TPC Chair of the EuCAP 2017 conference in Paris. He is also the Delegate of the French Research Ministry for the COST IC1102 action VISTA (Versatile, Integrated, and Signal-aware Technologies for Antennas) within the ICT Domain. He and his students received the H.W. Wheeler Award of the IEEE Antennas and Propagation Society for the best application paper of the year 2006. He was also the corecipient of the Jack Kilby Award 2013 of the ISSCC conference and the Best Paper Award of the EUCAP2007 conference, the Best Paper Award of the International Workshop on Antenna Technology (iWAT2009), the Best Paper Award at LAPC 2012, the Best Student Paper Award at LAPC 2013 (third place), the Best Paper Award of the ICEAA 2014 conference, and the Best Paper Award of the innovation contest of the iWEM 2014 conference (second place).

Gilles Jacquemod (M'xx) graduated from ICPI (CPE) Lyon, and received the M.Sc. degree (DEA) in microelectronics from Ecole Centrale Lyon, Écully, France, in 1986, the Ph.D. degree in integrated electronics from INSA Lyon, Lyon, France, in 1989.

From 1990 to 2000, he was with LEOM, Ecole Centrale Lyon, as an Associate Professor, on analog integrated circuit design and behavioral modeling of mixed domain systems. In 2000, he joined the LEAT Laboratory, Nice, France, the Ecole Polytechnique, Palaiseau, France, and Nice-Sophia Antipolis University, Nice, France, as a Full Professor. Since 2010, he has been with EpOC Research Team (URE UNS). He is the author and coauthor of more than 250 journal and conference papers, and holds 3 patents. His research interests include analog integrated circuit design and behavioral modeling of mixed domain systems. He is also involved in RF design applied to wireless communication.

Dr. Jacquemod is the Director of the CNFM PACA pole. He was the President of the CIM-PACA Design Platform.

Romain Pilard (M'xx) received the B.S. and M.S. degrees in electronics engineering from Polytech'Nantes, University of Nantes, Nantes, France, in 2006, and the Ph.D. degree in electrical engineering from Telecom Bretagne, Brest, France, in 2009.

Since 2010, he has been with the STMicroelectronics, Crolles, France, where he works on the development of integrated antennas and high-performance passive components in advanced bulk and SOI RF CMOS technologies. His research interests include millimeter-wave antenna design and packaging technology development.

Frédéric Gianesello (M'xx) received the B.S. and M.S. degrees in electronics engineering from the Institut National Polytechnique de Grenoble, Grenoble, France, in 2003 and the Ph.D. degree in electrical engineering from the Joseph Fourier University, Grenoble, France, in 2006.

He is currently working for STMicroelecetronics, Crolles, France, where he leads the team responsible for the development of electromagnetic devices (inductor, balun, transmission line, and antenna) integrated on advanced RF CMOS/BiMOS (down to 14 nm), silicon photonics, and advanced packaging technologies (3-D Integration, FOWLP, etc.). He has authored and coauthored more than 110 refereed journal and conference technical articles.

Dr. Gianesello has served on the TPC for the International SOI Conference from 2009 up to 2011 and he is currently serving on the TPC for the Loughborough Antennas and Propagation Conference (LAPC).

Jorge R. Costa (S'97–M'03–SM'09) was born in Lisbon, Portugal, in 1974. He received the Licenciado and Ph.D. degrees in electrical and computer engineering from the Instituto Superior Técnico (IST), Technical University of Lisbon, Lisbon, Portugal, in 1997 and 2002, respectively.

He is currently a Researcher with the Instituto de Telecomunicações, Lisbon, Portugal. He is also an Associate Professor with the Departamento de Ciências e Tecnologias da Informação, Instituto Universitário de Lisboa (ISCTE-IUL), Lisbon, Portugal. He is the coauthor of four patent applications and more than 100 contributions to peer reviewed journals and international conference proceedings. More than twenty of these papers have appeared in IEEE Journals. His research interests include lenses, reconfigurable antennas, MEMS switches, UWB, MIMO, and RFID antennas.

Prof. Costa is currently serving as an Associate Editor for the IEEE TRANSACTIONS ON ANTENNAS AND PROPAGATION and he was a Guest Editor of the Special Issue on "Antennas and Propagation at mm- and Sub mm-Waves," from the IEEE TRANSACTIONS ON ANTENNAS AND PROPAGATION, April 2013. He was the Co-Chair of the Technical Program Committee of the European Conference on Antennas and Propagation (EuCAP 2015) in Lisbon.

Carlos A. Fernandes (S'86–M'89–SM'08) received the Licenciado, M.Sc., and Ph.D. degrees in electrical and computer engineering from Instituto Superior Técnico (IST), Technical University of Lisbon, Lisbon, Portugal, in 1980, 1985, and 1990, respectively.

He joined IST in 1980, where he is currently a Full Professor with the Department of Electrical and Computer Engineering in the areas of microwaves, radio wave propagation and antennas. He is a Senior Researcher with the Instituto de Telecomunicações and member of the Board of Directors. He has coauthored a book, a book chapter, more than 150 technical papers in peer-reviewed international journals and conference proceedings and 7 patents in the areas of antennas and radiowave propagation modeling. His research interests include dielectric antennas for millimeter wave applications, antennas, and propagation modeling for personal communication systems, RFID and UWB antennas, artificial dielectrics, and metamaterials.

Dr. Fernandes was a Guest Editor of the Special Issue on "Antennas and Propagation at mm- and Sub mm-Waves," from the IEEE TRANSACTIONS ON ANTENNAS AND PROPAGATION, April 2013.

Eduardo B. Lima (S'14) received the Licenciado and M.Sc. degrees in electrical and computer engineering from the Instituto Superior Técnico (IST), Technical University of Lisbon, Lisbon, Portugal, in 2003 and 2008, respectively. He is currently working toward the Ph.D. degree at IST.

He is also currently a Researcher with the Instituto de Telecomunicações (IT), Lisbon, Portugal. Since 2004, he has been also responsible for development and maintenance of all measurement control systems at the RF laboratories. He is the coauthor of one patent application and 32 technical papers in international journals and conference proceedings in the area of antennas. One of which was awarded the CST University Publication Award 2010. His research interests include dielectric lens antennas, Fabry–Pérot cavity antennas, and transmit arrays.

Dr. Lima is currently serving as a Technical Reviewer for the IEEE TRANSACTIONS ON ANTENNAS AND PROPAGATION (TAP) and he also served as a TPC member in the EuCAP2015 conference.

Chinthana J. Panagamuwa (M'xx) received the Master of Engineering (M.Eng.) degree in electronic and electrical engineering and the Ph.D. degree in electronic and electrical engineering from Loughborough University, Loughborough, U.K., in 2000 and 2005, respectively.

Since 2007, he has been a Lecturer in Photonic Systems with the Wolfson School of Mechanical, Manufacturing, and Electrical Engineering, Loughborough University. His research interests include optically activated semiconductor switches for microwave circuits, devices and antennas. He also conducts research on specific absorption rates due to mobile communications devices and in-body antennas.

Since 2011, he is the Coordination Chair of the Loughborough Antennas and Propagation Conference series.

William G. Whittow (M'12–SM'12) received the B.Sc. degree in physics and the Ph.D. degree in computational electromagnetics from the University of Sheffield, Sheffield, U.K., in 2000 and 2004, respectively.

From 2004 to 2012, he was a Research Associate with the School of Electronic, Electrical and Systems Engineering, Loughborough University, Loughborough, U.K. He was a Lecturer in Electronic Materials Integration, University of Loughborough, in 2012 and he became a Senior Lecturer in May 2014. He has authored more than 150 peer-reviewed journal and conference papers in topics related to electromagnetic materials, synthetic dielectrics, wearable antennas, VHF antennas, specific absorption rate, FDTD, bioelectromagnetics, meta-materials, heterogeneous substrates, embroidered antennas, inkjet printing, electromagnetic compatibility, phantoms and Genetic Algorithms.

Dr. Whittow was the Coordinating Chair of the Loughborough Antennas and Propagation Conference (LAPC). He is an Associate Editor of *Electronics Letters*. He serves on the technical programme committees of several IEEE international conferences. He has been asked to give 6 invited conference presentations and a 4-day invited workshop on bioelectromagnetics.

QUERIES

Q1: Please provide postal code for all the affiliations.
Q2: Please provide author name and year of publication for Refs. [1]–[5], and [14].
Q3: Please provide page range for Ref. [11].
Q4: Please provide complete details for Ref. [15].
Q5: Please provide membership history (year) for authors “Aimeric Bisognin, Cyril Luxey, Gilles Jacquemod, Romain Pilard, Frédéric Gianesello, and Chinthana J. Panagamuwa.”
Q6: Please provide field of study for Master’s and Ph.D. degrees of author “Aykut Cihangir.”
Q7: Please provide location for Aerospace Industry in the biography section.

Ball Grid Array-Module With Integrated Shaped Lens for WiGig Applications in Eyewear Devices

Aimeric Bisognin, *Student Member, IEEE*, Aykut Cihangir, Cyril Luxey, *Senior Member, IEEE*, Gilles Jacquemod, *Member, IEEE*, Romain Pilard, *Member, IEEE*, Frédéric Gianesello, *Member, IEEE*, Jorge R. Costa, *Senior Member, IEEE*, Carlos A. Fernandes, *Senior Member, IEEE*, Eduardo B. Lima, *Student Member, IEEE*, Chinthana J. Panagamuwa, *Member, IEEE*, and William G. Whittow, *Senior Member, IEEE*

***Abstract*—A ball grid array-module (BGA-module) incorporating a low-cost shaped dielectric lens is proposed for wireless communications in the 60-GHz WiGig band between a smart eyewear, where it is integrated and facing a laptop or TV. The module, which is codesigned with a 60-GHz transceiver, consists of two separate identical antennas for transmitting (Tx) and receiving (Rx). The in-plane separation of these elements is 6.9 mm both being offset from the lens focus. This poses a challenge to the lens design to ensure coincident beam pointing directions for Rx and Tx. The shaped lens is further required to narrow the angular coverage in the elevation plane and broaden it in the horizontal plane. A 3-D-printed eyewear frame with an integrated lens and a recess for proper BGA-module integration is fabricated in ABS-plastic material. Measurements show a reflection coefficient below −12 dB in the 57–66 GHz band. A maximum gain of 11 dBi is obtained at 60 GHz, with 24° and 96° beamwidth at 5-dBi gain, respectively, in the vertical and horizontal planes. The radiation exposure is evaluated for a homogeneous SAM head phantom and a heterogeneous visible human head. The simulated power density values for both models are found to be lower than the existing standards.**

***Index Terms*—60 GHz, antenna-in-package, eyewear, lens antennas, plastic packaging, WiGig.**

I. Introduction

WITH the never-ending improvement of the capabilities of wireless communication devices, the most critical necessity has been to supply the user with higher and higher data rates. This has led to both the improvement of the existing wireless communication standards as well as the launch of new standards and new technologies. One of these standards, the WiGig IEEE 802.11ad, is gaining more and more popularity among industries because the unlicensed frequency band around 60 GHz offers a broad bandwidth to achieve multigigabits speeds (up to 7 Gbit/s). The low interference level favored by the very high wall penetration loss and by the high oxygen absorption in this band for moderate distances makes this standard a good candidate for line-of-sight (LoS) in-room wireless personal area communications (WPAN). Possible applications include the wireless connection of a personal computer (PC) with its peripheral devices (monitor, keyboard, etc.), as well as ultra-high-definition video/audio transfer from a camera to a TV or projector, eliminating the need for cables. Typically, for a LoS 2-meter communication in this band, an antenna gain of approximately 4 dBi is needed (at both sides of the link) considering today's transceiver performances (10 dBm power at the antenna port, −54 dBm Rx sensitivity and OFDM 16-QAM modulation). If this distance is increased to around 8 m, the gain should be approximately 10 dBi.

In parallel, smart eyewear devices are gaining popularity as wireless communicating objects with some products already released in the market and some other being prepared for the near future [1]–[5]. In general, those devices incorporate a small optical lens-reflector screen, a camera, a microphone/speaker pair, and a touchpad. They are generally connected to a peripheral (smartphone or set-top box) through Bluetooth or WLAN standards at 2.4 GHz. Our recent work considered eyewear devices as a possible candidate to replace smartphones in the near future and we successfully demonstrated high potential for LTE communications [6].

In this study, a ball grid array-module (BGA-module) incorporating separate Tx and Rx antennas (to avoid a lossy switch at 60 GHz in TDD mode) integrated with a shaped 3-D-printed plastic lens is proposed for integration with a smart eyewear device for high-speed video transfer from the device to a laptop or a TV in front of the user. The transceiver is based on an RFIC design using 65 nm CMOS technology and aims to fulfill the WiGig requirements for its highest available data rate, i.e., MCS20. This mode offers a 4.158-Gbps data rate thanks to OFDM 16-QAM modulation. All WiGig frequency subbands are covered from 57 to 66 GHz. The chipset is described in detail in [7]. The shaped lens is intended to achieve an acceptable gain (> 10 dBi) and to shape the radiation pattern

Manuscript received November 16, 2014; revised November 05, 2015; accepted December 19, 2015. Date of publication XXXX XX, XXXX; date of current version XXXX XX, XXXX.

A. Bisognin is with EpOC, Université Nice Sophia Antipolis, Valbonne, France, and also with STMicroelectronics, Crolles, France.

A. Cihangir and G. Jacquemod are with EpOC, Université Nice Sophia Antipolis, Valbonne, France.

C. Luxey is with EpOC, Université Nice Sophia Antipolis, Valbonne, France, and also with Institut Universitaire de France (IUF), Paris, France (e-mail: cyril.luxey@unice.fr).

R. Pilard and F. Gianesello are with STMicroelectronics, Crolles, France.

C. Fernandes and E. Lima are with Instituto de Telecomunicações, Instituto Superior Técnico, University of Lisbon, Lisbon, Portugal.

J. Costa is with DCTI, Instituto Universitário de Lisboa (ISCTE-IUL), and Instituto de Telecomunicações, Lisbon, Portugal.

C. Panagamuwa and W. Whittow are with the Wireless Communications Research Group, School of Electronic, Electrical and Systems Engineering, Loughborough University, Loughborough, LE11 3TU, U.K. (e-mail: w.g.whittow@lboro.ac.uk, C.J.Panagamuwa@lboro.ac.uk).

Color versions of one or more of the figures in this paper are available online at http://ieeexplore.ieee.org.

Digital Object Identifier 10.1109/TAP.2016.2517667

with wide beamwidth in the horizontal plane (at least 100° at 5 dBi gain) and narrow beamwidth in the vertical plane (in the order of 25° at 5 dBi gain). The challenge for its design is the additional need to counteract the beam depointing effect due to the impossibility of positioning the separate Tx and Rx radiating elements simultaneously at the lens single focal point. The in-plane separation of these radiating elements is 6.9 mm. The lens was found to be a convenient solution to address the shaped beam challenge instead of using a large planar array with low aperture efficiency and nonuniform (and lossy) feeding network. The objective of the paper is to show that the proposed antenna concept is feasible for mm-wave eyewear applications, being compact, low cost and with negligible impact in terms of head specific absorption rate (SAR). Section II gives some basic information about the BGA-module and the Tx and Rx radiating elements. The design of the lens with its theoretical background and simulation results are also explained in this section. The integration of the BGA-module and the lens within the eyewear is presented in Section III. Simulation results taking into account the presence of the user's head are also presented in this section. Measurement results for the manufactured prototype are given in Section IV. Section V discusses the evaluation of the radiation exposure on the body through simulations. Finally, conclusion is drawn in Section VI.

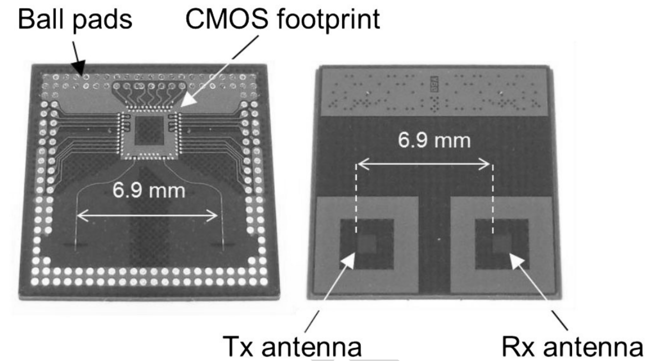

Fig. 1. Picture of the BGA-module version 2: bottom view on left and top view on right.

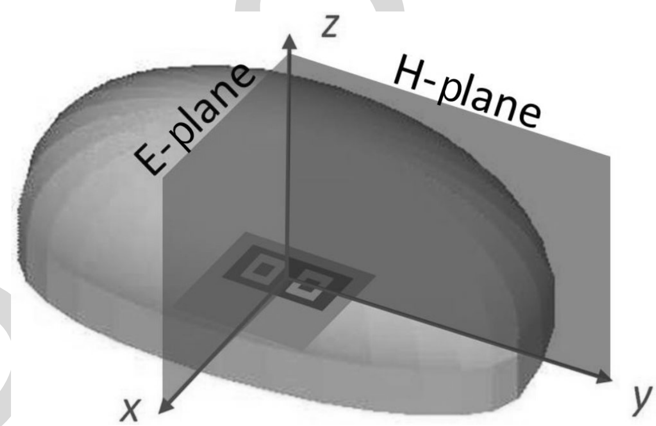

Fig. 2. Schematic view of the optimized 3-D-lens placed above the BGA-module with axis definition.

II. Antenna Design

A. BGA-Module

The BGA-module was designed and manufactured in high density integration (HDI) technology dedicated to 60 GHz SiP solutions. This HDI technology is based on standard BGA design and realization techniques: it enables a minimum trace resolution as well as trace spacing of $50~\mu$m. The low-cost stack-up of three organic substrates enables four metallization layers. A picture of the BGA-module can be seen in Fig. 1. This module was designed to radiate in free-space. The module has equal length and width (12×12 mm^2) with a height of 0.5 mm. It hosts two printed antennas, one for receiving and one for transmitting, offset from the center of the BGA-module and separated by $\Delta d = 6.9$ mm distance from each other ($1.38~\lambda_0$). The antennas are of aperture-coupled patch type, where the apertures are excited through a microstrip line underneath them. The antennas are linearly polarized with a measured gain higher than 4 dBi between 57 and 66 GHz (including transmission line losses). More information about the BGA-module (version 1) and the antenna can be found in [8]. They are thus not repeated here for the sake of brevity. However, it should be noted that a second optimized version of the BGA-module is used in the current paper having more than 10 dB return loss and 5 dBi gain from 57 to 66 GHz which is better than the performance presented in [8].

B. Lens Design

A small shaped lens is used directly on top of the patch elements of BGA-module to modify its radiation pattern into a more convenient shape for the intended application. The gain is required to exceed 5 dBi within a 100° angular interval in the horizontal plane (H-plane, or yz-plane in Fig. 2) and 25° angular interval in the vertical plane (E-plane or xz-plane in Fig. 2). This gives the user enough margin to look comfortably at the screen from different angles without compromising the data link. It should be noted that no codesign between the source and the lens was achieved as we reused the existing BGA-module version 2 dedicated to radiate in free space (and not plastic medium).

The radiation pattern described in the paragraph above is not symmetric and therefore requires a full 3-D shaped lens. Although geometrical optics (GO) formulations exist for the design of arbitrary shaped dielectric lenses subject to arbitrarily output power template conditions [9]–[10], it is shown in this study that for the present radiation pattern specifications it is enough to consider a far simpler and computationally fast alternative based on a modification of the GO formulation for axial symmetric lenses.

The combination with physical optics (PO) analysis enables faster optimization of the shape of the 3-D lens compared to the exact 3-D GO formulation, offering a very reasonable agreement with the targeted radiation pattern beamwidths.

The GO/PO-based lens design procedure requires prior knowledge of the radiation pattern of one antenna of the BGA-module into an unbound medium of the chosen material for

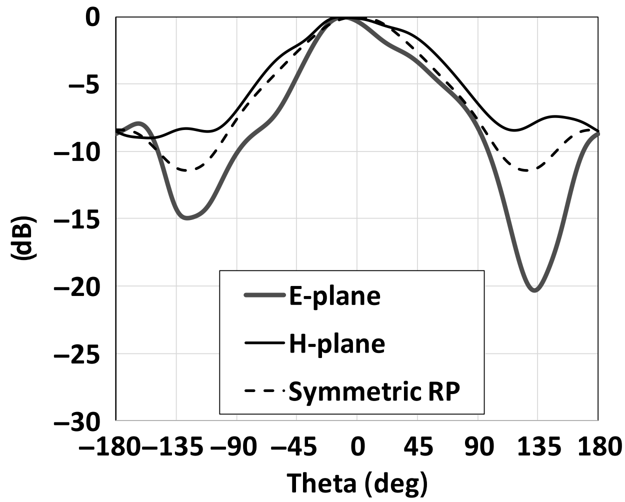

Fig. 3. Normalized simulated E- and H-plane radiation patterns of the BGA-module (Tx-antenna) in an unbounded medium of ABS plastic. Symmetric RP is an average of the E- and H-planes further used for the lens design.

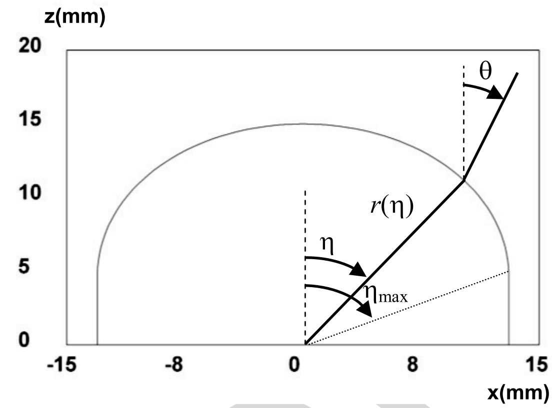

Fig. 4. Horizontal (or H-plane) profile of the plastic lens.

the lens. ABS-M30 plastic material (consumer grade plastic used for smartphone casing) was chosen in order to ensure low cost for the overall system. A 3-D-printing rapid manufacturing technology was selected to fabricate the lens. A disk sample of ABS material was printed to experimentally evaluate its complex permittivity. The Fabry–Perot resonator measurement method presented in [11] gave us $\epsilon_r = 2.48$ and $\tan(\delta) = 0.009$ at 60 GHz. The lens design was performed at 60 GHz, as the central frequency. Intrinsic to the GO design, the frequency bandwidth of the lens is inherently large but the full-system bandwidth is mainly determined by the BGA-module bandwidth. The radiation pattern of the feed inside the unbounded ABS medium at 60 GHz was obtained from a full-wave HFSS simulation (Fig. 3). Overall, the main E- and H-planes of the bare BGA antennas have similar beamwidths. The 3-D shaped lens is designed in two steps. First, the lens profile in the horizontal plane is obtained from an elevation cut of an axial-symmetric lens designed with an appropriate GO formulation. Then, the design rule for the lens profile in the vertical plane is defined and the complete 3-D lens physical shape is obtained from an adequate combination of both horizontal and vertical lens profiles.

Fig. 4 shows the general geometry for the lens design procedure. The axial symmetric lens profile is represented by $r(\eta)$ where $r(\eta = 0°) = 15$ mm corresponds to the total height of the lens. The feed, corresponding to one patch of the BGA-module, is assumed initially to be at the center of the base of the lens and in direct contact with it. The lens design assumes that the feed is positioned at the center of the lens. However, the target radiation pattern $G(\theta)$ that is needed to define the lens shape is carefully optimized to minimize its dependence with feed offset when the BGA-module is integrated at the base of the lens. At this point, the lens design formulation requires that the feed radiation pattern $U(\eta)$ is axial symmetric. The symmetric $U(\eta)$ power pattern is generated as an average of the cocomponents in the main planes of the BGA antenna (symmetric RP curve in Fig. 3). The obtained $U(\eta)$ function is represented in Fig. 3 by the black dashed curve (symmetric RP). Other symmetrization options could have been adopted for the feed radiation pattern. They would imply different $r(\eta = 0)$ values and different $G(\theta)$ shape from what we obtained in the optimization process. The selected target pattern $G(\theta)$ is a flat-top type with a sharp drop-off at $\theta = 60°$ to comply with the desired full 100° beamwidth in the horizontal plane of the lens.

The lens profile $r(\eta)$ is designed to transform $U(\eta)$ into a target axial symmetric power pattern $G(\theta)$. The $r(\eta)$ profile is obtained by solving a set of two differential equations defined by the authors in [12]. The integration is performed for increasing η angles up to the $\eta_{\max}$ value where $\partial r(\eta)/\partial\eta$ becomes negative. This $\eta_{\max}$ angle defines the edge of the lens (Fig. 4). The remaining points in the lens profile from $z = r(\eta_{\max})\ \cos(\eta_{\max})$ to $z = 0$ are defined with a constant value of $x = r(\eta_{\max})\ \sin(\eta_{\max})$. By forcing nonnegative $\partial r(\eta)/\partial\eta$, the lens surface will not diffract the radiation of the feed into the negative z direction, i.e., into the user. The analytical formulation is valid for arbitrary initial values $r(\eta = 0°)$ which acts as a scaling factor. In the axial symmetric lens, the matching between the output power pattern and the horizontal plane target improves as $r(\eta = 0°)$ increases. This value influences the vertical plane power pattern in a different way, as will be discussed ahead. In the present design, $r(\eta = 0°) = 15$ mm was chosen as a compromise between the output power pattern specification in both planes and the utmost size constraint for the desired integration with the glasses. The obtained lens profile is presented in Fig. 4. This curve is used as the horizontal profile of the 3-D lens. In the vertical plane (E-plane), narrowing the radiation pattern of the BGA-module can be achieved by using a beam collimating lens profile (like an ellipse). For each cut of the 3-D lens at a constant x value, an elliptical lens profile is implemented (Fig. 5). Each x-cut corresponds to a given η angle so that $x = r(\eta)\sin(\eta)$. In each x-cut, the height of the elliptical profile is $F(\eta) = r(\eta)\cos(\eta)$. The elliptical lens profile is defined by

$$l(\eta, \alpha) = \frac{\sqrt{\varepsilon_r} - 1}{\sqrt{\varepsilon_r} - \cos(\alpha)} F(\eta) \tag{1}$$

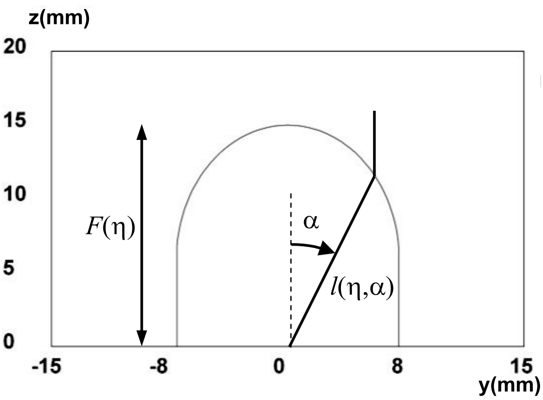

Fig. 5. Vertical cut of the plastic lens profile for a x = constant plane.

where α is the angle of each point $l(\eta,\alpha)$ in relation to the vertical axis of each cut plane of the lens profile as indicated in Fig. 5. Therefore, the complete 3-D lens profile is defined by the following set of parametric equations

$$\begin{aligned} x(\eta,\alpha) &= r(\eta)\sin(\eta) \\ y(\eta,\alpha) &= l(\eta,\alpha)\sin(\alpha) \\ z(\eta,\alpha) &= l(\eta,\alpha)\cos(\alpha). \end{aligned} \tag{2}$$

As with η, the α angle also ranges from 0 to $\alpha_{\max}$ where $\partial l(\eta\alpha)/\partial\alpha$ becomes negative. The remaining points from $z = z(\eta, \alpha_{\max})$ to $z = 0$ are defined with a constant $y = y(\eta, \alpha_{\max})$.

The obtained 3-D lens profile is shown in Fig. 2. Its overall size is $\Delta z = 15$ mm by $\Delta x = 26$ mm and $\Delta y = 14$ mm. This approximate 3-D lens design procedure is an evolution of the one developed by the authors in [13]. The corresponding radiation pattern is calculated using PO, considering the actual nonsymmetric feed radiation pattern shown in Fig. 3.

The normalized result is presented in Fig. 6(a) for the main planes, confirming the effectiveness of the proposed design. The simulated maximum directivity is of the order of 12 dBi. To achieve a narrower E-plane radiation pattern and a higher lens directivity, the lens size can be increased by choosing a higher value for $r(\eta = 0°)$.

Due to the Rx and Tx $\Delta d = 6.9$ mm separation in the BGA-module, the lens is not fed from its focal point at the center of the base of the lens. The $\Delta d/2 = 3.45$ mm (0.69 λ_0 at 60 GHz) feed off-set in the x-axis tends to produce a beam depointing effect. However, the previous H-plane radiation pattern template was specifically chosen to minimize this effect. It is noted that the y-plane elliptical profile does not allow depointing minimization if y-axis feed off-set was selected instead. The x-axis feed off-set effect in the horizontal plane (H-plane) radiation pattern of the lens can be seen in Fig. 6(b), showing that the flat-top characteristic is reasonably maintained and only 1 dB reduction is observed in the broadside direction from the nonoffset source case. It has little influence in the E-plane since Tx and Rx patches remain in the focal point of the elliptical x-cut profile of the lens that passes through each feed position.

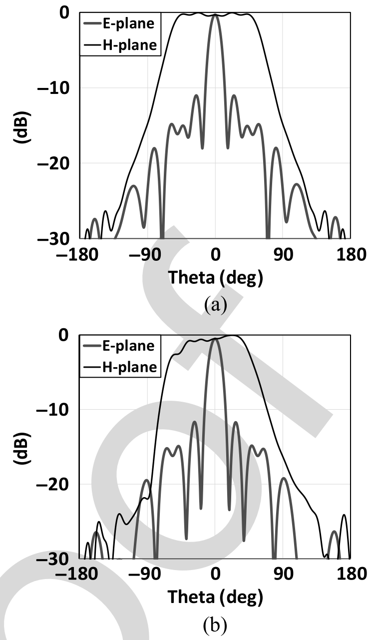

Fig. 6. Normalized GO/PO simulated radiation pattern of the 3-D lens fed by the Tx patch of the BGA-module at 60 GHz. (a) Feed at the center of the lens. (b) Feed offset from the center by x = 3.45 mm.

III. Integration of the BGA-Module With the Eyewear Device

In order to validate the GO/PO-based lens design and to evaluate the antenna in the realistic use-case scenario, full wave electromagnetic simulations were also carried out, using the commercial software Empire XCcel [14]. The simulation model included the BGA-module integrated with the dielectric lens, mounted in the left-hand side of a dedicated ABS eyewear frame (Fig. 7 left part). An FR4 substrate which might be needed in a realistic product as the application PCB and a backing ground plane was also included in this model, behind the antenna-module (Fig. 8). The frame includes a curved region on the right-hand side of the head to emulate visually the screen of a smart eyewear device. It also includes on the two sides of the frame, two parallelepiped casing-like structures for housing the application PCBs for WLAN/Bluetooth and WiGig standards, respectively.

A homogeneous specific anthropomorphic mannequin (SAM) head was also included in the simulation to account for the user head influence. Considering the computation time and memory requirements to simulate the full set-up from Fig. 7, it was decided to use a cropped model of the head, since the effects of the tissues that are placed far from the antenna in terms of wavelength will be negligible. The cropped model used in the simulations can be seen in Fig. 7 (right side). It keeps all the structures and materials that lie within 10 λ_0 distance from the Antenna-module and discards all the others, so the final dimensions of the simulation rectangular box is $78 \times 73 \times 155$ mm^3. The lens and the dielectric frame were modeled as ABS plastic material. The values taken from Fabry–Perot measurements and given in Section II B were used to

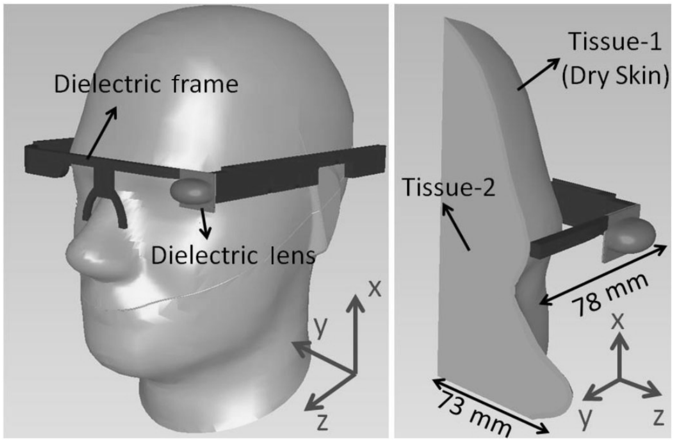

Fig. 7. Simulation model of the BGA-module integrated with the lens and the ABS eyewear frame close to the SAM Head. The shaped lens is on the frame left side.

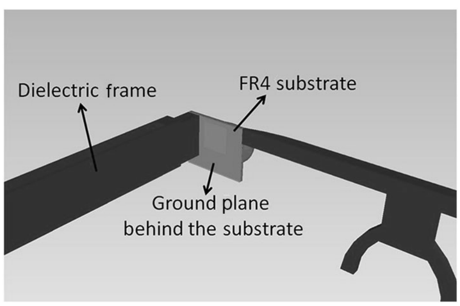

Fig. 8. Position of the FR4 substrate and the ground plane which is backing the antenna-module.

model the ABS material. The outer shell of the head (marked as Tissue-1) was assigned the properties of dry skin at 60 GHz, having a relative permittivity of 7.98 and a loss tangent of 1.37. To model the interior region of the head (Tissue-2), electrical properties of the brain was used, with a relative permittivity of 10.4 and loss tangent of 1.19. Those values were taken from [15].

A second set of simulations was also performed removing the head and the backing PCB of the lens. The comparison of the simulated reflection coefficient of the Tx antenna of the BGA-module with the lens without the head and PCB and with the head and PCB is presented in Fig. 9. The simulated coupling coefficient from the Tx antenna to Rx antenna is very low ($|S_{21}| < -30$ dB) and thus is not shown here. The Tx antenna integrated with the lens with the backing PCB and head has a reflection coefficient always lower than -6.7 dB between 57 and 66 GHz, even decreasing below -15 dB around the lower edge of the band. It can also be seen from the same figure that the reflection coefficient of the same Tx antenna without backing PCB and head is very similar, suggesting negligible effects of the head and the backing PCB. The consequence of the absence of a codesign between the source and the lens directly translates into a frequency shift (compared to the "without head and PCB case") with a minimum of $|S_{11}|$ around 55–57 GHz (almost out-of-band) as the BGA-module now radiates into plastic rather than air.

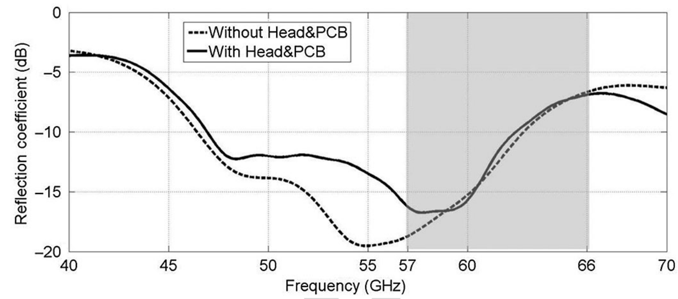

Fig. 9. Simulated reflection coefficient for the Tx patch of the BGA-module integrated with the lens without the Head and PCB and with the Head and PCB.

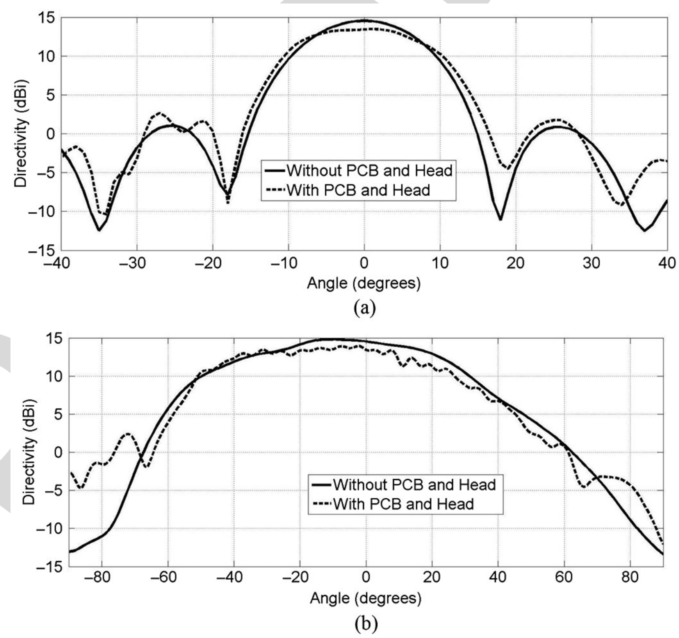

Fig. 10. Full-wave simulated directivity patterns of the BGA-module integrated with the lens with head and PCB and without head and PCB. (a) E-plane and (b) H-plane at 60 GHz.

The comparison of the full-wave radiation patterns in the E-plane ($\varphi = 0°$) and H-plane ($\varphi = 90°$) for the two configurations is shown in Fig. 10(a) and (b), respectively. The maximum radiation does not occur exactly in the front direction of the eyewear. There is a slight asymmetry in the radiation pattern (10° tilt) but this is not really important in this application as the beam tilt is small as compared to the beamwidth and the user does not necessarily have to be directly in front of the receiving device. Note that the obtained radiation patterns confirm that the lens geometry is fairly suitable to overcome the focal depointing. In addition, the specified 5 dBi gain beamwidth of 25° in the E-plane and 100° in the H-plane is very closely met. The maximum full-wave simulated directivity is almost 15 dBi which is higher than the 12 dBi simulated with GO/PO. We anticipate that the difference is mainly the result of known limitations of the GO/PO asymptotic method for small-size lenses. Also, it is known that a surface wave may appear for elliptical lenses at the lens/air interface which, for some lens sizes, can lead to higher directivity than predicted with GO/PO [16]. The head and the PCB behind the antenna-module have little

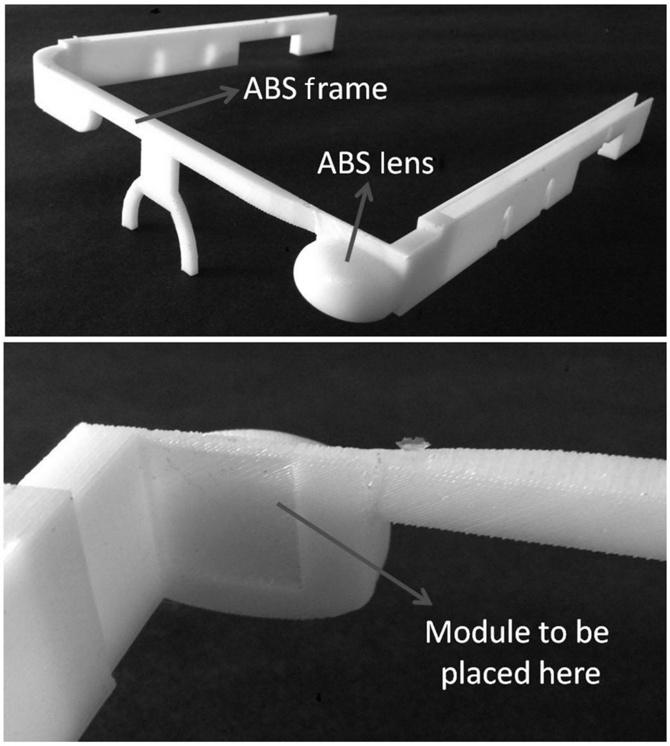

Fig. 11. Pictures of the manufactured ABS frame incorporating the shape of the lens.

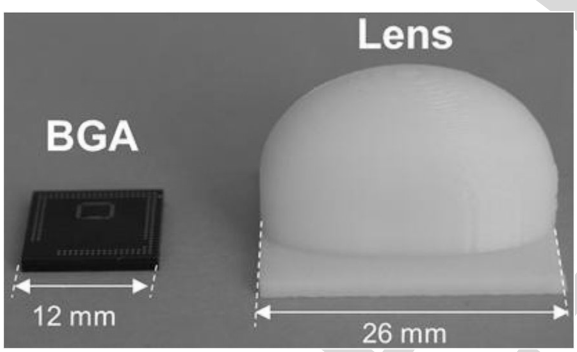

Fig. 12. BGA-module and 3-D-printed ABS plastic lens.

effects (but not significant) in the general radiation pattern (1 dB reduction of the directivity and broader beam is the E-plane); however, we decided to omit this last configuration in the next simulation studies and measurements.

IV. Measurements

A. Fabrication of the Eyewear Prototype and the Antenna-Module

A picture of the manufactured ABS frame integrating the lens is shown in Fig. 11. Fig. 12 presents the BGA-module (left side) and the ABS lens alone (right side). All the ABS prototypes were fabricated using 3-D printing plastic technology.

B. Measurement Results

The measurements of the BGA-module with the integrated lens were carried out without the head and PCB, following the

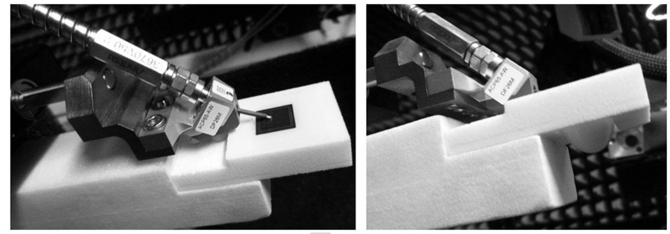

Fig. 13. Pictures of the probing of the Tx antenna of the BGA-module with the lens (left side), bottom view of the BGA-module with the lens inside the foam support (right side).

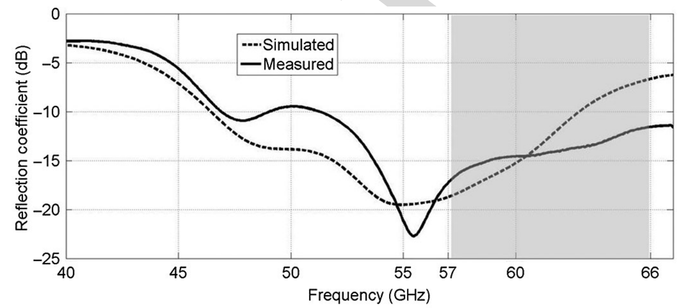

Fig. 14. Simulated and measured reflection coefficient of the Tx antenna of the BGA-module with the lens.

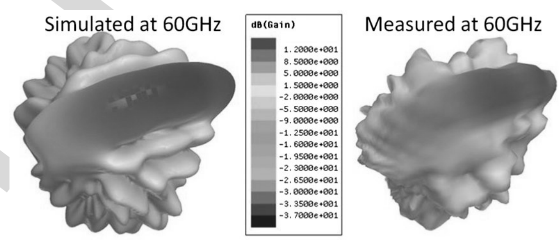

Fig. 15. Simulated and measured 3-D realized gain patterns of the BGA-module with the lens at 60 GHz.

conclusion from the previous section. Also, the full eyewear frame was not utilized for the radiation pattern measurements as it physically impairs the access of the feeding probe used in our millimeter-wave measurement set-up [17] (Fig. 13).

There is a good agreement between measured and simulated reflection coefficients given in Fig. 14. The measured reflection coefficient is well below -11.5 dB in the target band (57–66 GHz). Note, no codesign was performed which suggests that better performance could be achieved in a possible new version of the eyewear and BGA-module. The simulated and measured realized gain patterns are presented in 3-D form in Fig. 15 and in the main planes in Fig. 16(a) (E-plane for $\varphi = 0°$) and Fig. 16(b) (H-plane for $\varphi = 90°$). The maximum measured gain is approximately 11 dBi at 60 GHz (including the transmission line losses). The measured 5 dBi gain beamwidth is 24° in E-plane and 96° in H-plane. A comparison of the simulated and measured radiation efficiency can be seen in Fig. 17. A fair agreement is observed, especially in the target band between 57 and 66 GHz. The measured efficiency has been extracted from the 3-D realized gain pattern with the method already presented in [18]. The Tx antenna of the BGA-module has a measured radiation efficiency ranging from 52% to 58% in this band which is a suitable value for WiGig transmissions between

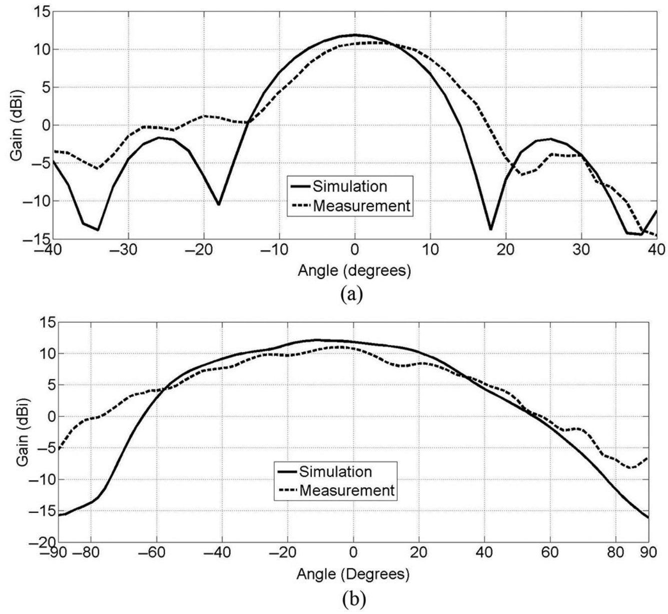

Fig. 16. Simulated and measured realized gain of the BGA-module with the lens in (a) E-plane and (b) H-plane at 60 GHz.

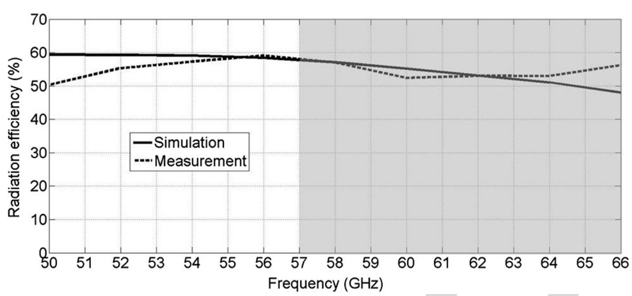

Fig. 17. Simulated and measured radiation efficiency of the Tx antenna from the BGA-module with the lens.

the eyewear and a TV or a laptop. The stability of the gain pattern versus frequency was also investigated through the band of interest. Fig. 18 presents the measured realized gain patterns (E- and H-planes) for three frequency points: 58, 60, and 66 GHz. These patterns show negligible variation with respect to frequency even in terms of 5 dBi beamwidth as presented in Table I, all complying with the beamwidth specification.

V. Human Body Exposure

International standards based on the incident power density have been developed to limit the electromagnetic exposure by the human body from RF devices at 60 GHz. The IEEE (USA) recommends a maximum power density of $10\ \mathrm{W/m^2}$ averaged over $0.01\ \mathrm{m^2} (10\ \mathrm{cm} \times 10\ \mathrm{cm})$ averaged over 3.6 min for the general public [19]. The limit is $100\ \mathrm{W/m^2}$ in controlled environments averaged over 21.6 s [19]. The standards also determine a maximum power density of $1000\ \mathrm{W/m^2}$ averaged over any one square centimeter. ICNIRP (Europe) has power density limits of, respectively, $10\ \mathrm{W/m^2}$ and $50\ \mathrm{W/m^2}$ averaged over $20\ \mathrm{cm^2}$ for the general public and controlled conditions.

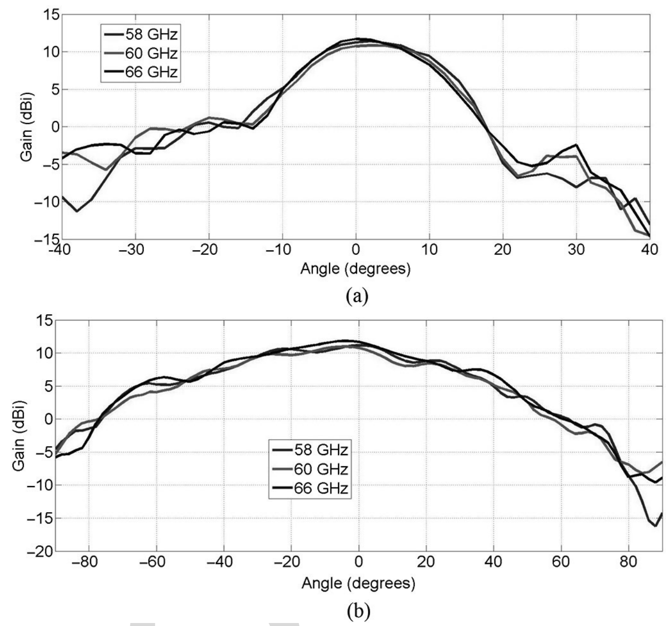

Fig. 18. Measured realized gain in (a) E-plane and (b) H-plane of the Tx antenna of BGA-module with the lens for different frequencies.

TABLE I
Comparison of Measured Beamwidth at Different Frequencies

	58 GHz	60 GHz	66 GHz	Target
E-plane 5 dBi BW	25°	24°	23°	25°
H-plane 5 dBi BW	106°	96°	108°	100°

The maximum power density averaged over $1\ \mathrm{cm^2}$ should not exceed 20 times the above values. The averaging time can be calculated by $68/\mathrm{f}1.05 = 0.92$ min. The ICNIRP levels are stricter for both the larger averaging areas and also the $1\ \mathrm{cm^2}$ area. Therefore, compliance with ICNIRP guarantees compliance with the IEEE recommendation. Despite the power density being defined in the standards, there is no consistent evaluation metric in the recent published papers. The local specific absorption rate (SAR) is examined in [20] and [21]. The 1-g SAR and the power absorbed were discussed in [22]. The maximum electric field, power density, and local SAR were assessed in [23]. *In vitro* protein and culture were considered in [24] and [25] where the maximum local SAR and the SAR averaged over the whole sample was related to the incident power density. A thermal imaging camera was used to measure the temperature distribution and hence the local and average power density as well as the local SAR in [26]. This paper concluded that power levels up to 550 mW would comply with the exposure limit and an incident power density of $10\ \mathrm{W/m^2}$ would result in a temperature increase of $0.1^\circ\mathrm{C}$.

In our study, two sets of simulations were performed for analyzing the effect of the BGA-module with lens on the head of the user. The first set of simulations was performed with a homogeneous head model as used in Section III, consisting of the outer part modeled as dry skin and the inner part modeled as the brain tissue. The second set of simulations was performed

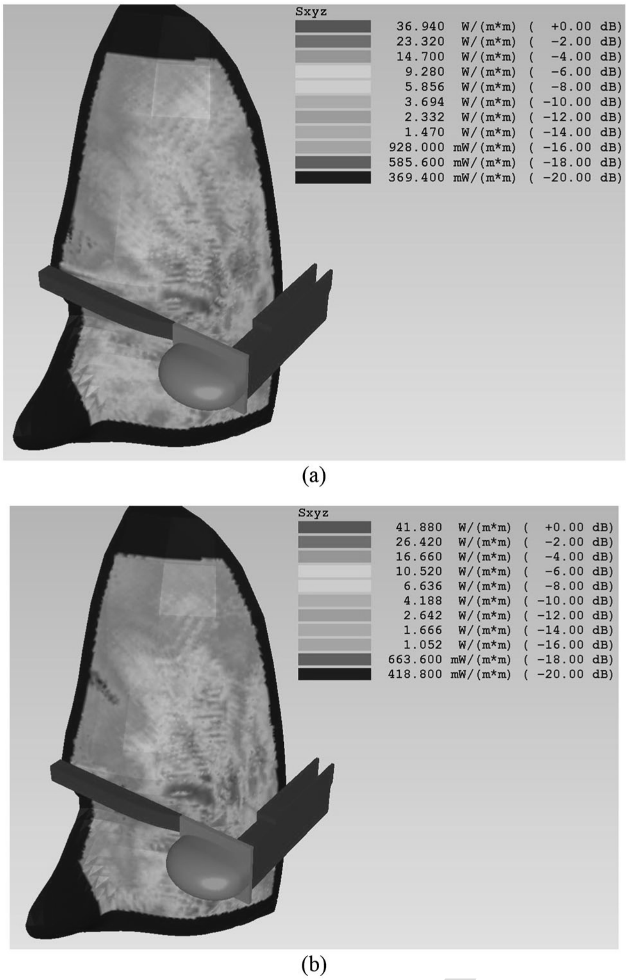

Fig. 19. Simulated power density with SAM head (scaled to 1 W input power) over the skin for (a) 60 GHz and (b) 66 GHz.

with the visible human head model taking into account different tissues with corresponding electrical properties.

A. Simulations With Homogeneous Head Model

Simulations with the homogeneous head model were performed to obtain the power density level at the surface of the skin. According to ICNIRP guidelines, the power density level on the tissue, averaged over 20 cm^2 should be lower than 1 mW/cm^2 (or 10 W/m^2) around 60 GHz frequency. The simulated power density with EMPIRE XCcel software on the skin surface can be observed in Fig. 19 for 60 and 66 GHz. It should be noted here that the values presented in this figure legends are not averaged either over time or space, so they are the worst-case levels. Moreover, the input power to the antenna was set as 1 W in the simulations so the power density levels shown in this figure need to be divided by 100 to comply with the typical input power level of 10 dBm for WiGig devices. The unaveraged maximum power density observed on the skin surface varies between 0.37 and 0.42 W/m^2 between 60–66 GHz (for an input power of 10 dBm). These values are well below the reference values from the guidelines even though they are instantaneous, unaveraged values. Obtaining such a low-power density over the skin was expected since the main radiation is directed away from the head and also the spacing between the antenna-module and the head is 30 mm which is 6 λ_0 at 60 GHz.

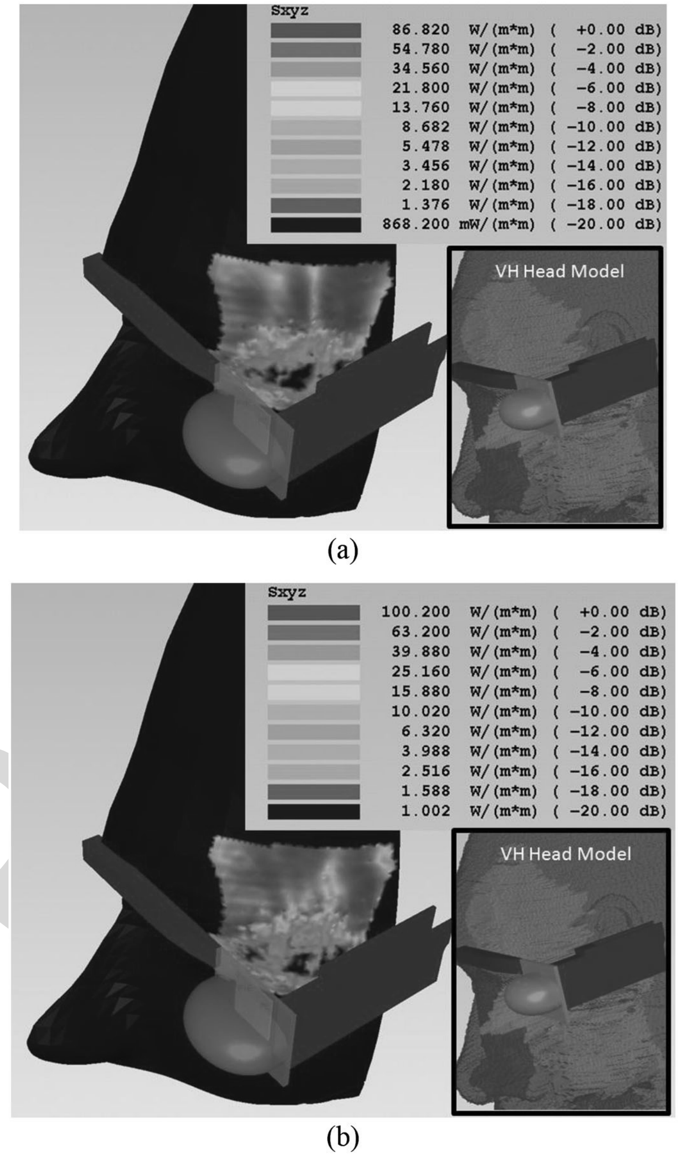

Fig. 20. Simulated power density with VH head (scaled to 1 W input power) for (a) 60 GHz and (b) 66 GHz.

B. Simulations With Visible Human Head Model

The simulations were also performed by placing the BGA-module with lens on a truncated VH model with 1 mm resolution (inset in Fig. 20). The Yee cell size inside the head was set to 0.2 mm and even smaller cells were used to discretize the BGA-module including the lens. Empire can display the power density on the surface of the SAM head, which is categorized as a solid shape, but not on the voxel-based VH head. Therefore, to examine the power density on the surface of the VH head, the SAM-shaped field monitor was copied to the VH simulation file. This allowed us to observe that the surface of the VH head was closer to the antenna than the SAM head. Therefore, the SAM-shaped field monitor was moved several millimeters toward the antenna to lie on the surface of the VH head. Approximate calculations using the path loss equation indicated that this positioning difference can increase the power density by approximately 5 dB. The power density on the surface of the VH head varies between 67 and 100 W/m^2 as shown in Fig. 20. These values are again the maximum values seen at a point in space, normalized to 1 W input power, without any space or time averaging. Considering 10nbsp;dBm of maximum input power in WiGig applications, the values are well below the standard values, even without averaging.

VI. Conclusion

This paper demonstrated the feasibility of a compact low-cost antenna assembly for a WiGig smart eyewear device intended for high-speed wireless data communication in the 60-GHz band with a laptop or TV facing the user. The antenna-module incorporates a 3-D-printed shaped dielectric lens especially designed to enhance gain while shaping the radiation pattern to provide wide angular coverage in the horizontal plane and narrow beam coverage in the vertical plane. The lens design was based on GO/PO but full wave electromagnetic simulation was carried out to evaluate the antenna assembly performance when integrated with the eyewear device. Results were presented for two scenarios: the first one included the user's head as well as a portion of a PCB backing the antenna-module. In the second scenario, the head and PCB were removed. It was demonstrated that the effect of the head and of the backing PCB on the radiation pattern and the reflection coefficient was negligible. Keeping this in mind, the measurements for the BGA antenna-module and the lens were carried out in free-space, showing a good agreement with the simulations in terms of reflection coefficient, radiation efficiency, and realized gain radiation pattern. The maximum measured gain at 60 GHz was 11 dBi, with 5 dBi gain beamwidth of 24° in the vertical plane and 96° in the horizontal plane (including the transmission line losses). The measured gain radiation pattern was also shown to have negligible variation over the target frequency band (57–66 GHz).

The effects of the antenna radiation on the human body was analyzed for two sets of simulations, using both a homogeneous SAM head phantom and visible human head model. The simulated power density values for both head models were found to be lower than the limits established in the related standards, considering an input power of 10 dBm.

Acknowledgment

The authors would like to acknowledge Orange Labs La Turbie and the CIM-PACA design platform. F. Devillers from Orange Labs is deeply acknowledged for the adjustments of the mechanical parts of the measurement set-up. They would also like to acknowledge a scholarship given by project ESF RNP "Newfocus" to Aimeric Bisognin.

References

[1] *Google Glass* [Online]. Available: http://www.google.com/glass/start/ Q2
[2] *M100 Smart Glass* [Online]. Available: http://www.vuzix.com/UKSITE/consumer/products_m100.html
[3] *RECON Jet* [Online]. Available: http://www.reconinstruments.com/products/jet/
[4] *Olympus MEG4.0* [Online]. Available: http://www.olympus.co.jp/jp/news/2012b/nr120705meg40j.jsp
[5] *Optinvent ORA* [Online]. Available: http://optinvent.com/see-through-glasses-ORA
[6] A. Cihangir *et al.*, "Feasibility study of 4G cellular antennas for eyewear communicating devices," *IEEE Antennas Wireless Propag. Lett.*, vol. 12, pp. 1704–1707, 2013.
[7] A. Siligaris *et al.*, "A 65 nm CMOS fully integrated transceiver module for 60 GHz wireless HD applications," *IEEE J. Solid-State Circuits*, vol. 46, no. 12, pp. 162–164, Dec. 2011.
[8] R. Pilard *et al.*, "HDI organic technology integrating built-in antennas dedicated to 60 GHz SiP solution," in *Proc. IEEE Antennas Propag. Soc. Int. Symp. (AP-SURSI)*, Chicago, IL, USA, Jul. 2012, pp. 8–14.
[9] C. Salema, C. A. Fernandes, and R. K. Jha, *Solid Dielectric Horn Antennas*. Norwood, MA, USA: Artech House, 1998.
[10] R. Sauleau and B. Bares, "A complete procedure for the design and optimization of arbitrarily shaped integrated lens antennas," *IEEE Trans. Antennas Propag.*, vol. 54, no. 4, pp. 1122–1133, Apr. 2006.
[11] C. A. Fernandes and J. R. Costa, "Permittivity measurement and anisotropy evaluation of dielectric materials at millimeter-waves," in *Proc. IMEKO World Congr.*, Lisboa, Portugal, Sep. 2009. Q3
[12] C. A. Fernandes, "Shaped dielectric lenses for wireless millimeter-wave communications," *IEEE Antennas Propag. Mag.*, vol. 41, no. 5, pp. 141–150, Oct. 1999.
[13] C. A. Fernandes, "Design of shaped lenses for non-symmetric cells in MBS," in *Proc. IEEE Antennas Propag. Soc. Int. Symp. (AP-S/URSI)*, Orlando, FL, USA, Jul. 1999, vol. 3, pp. 2440–2443.
[14] *EMPIRE XCcel* [Online]. Available: http://www.empire.de/
[15] [Online]. Available: http://www.itis.ethz.ch/itis-for-health/tissue-properties/database/tissue-frequency-chart/ Q4
[16] D. Pasqualini and S. Maci, "High-frequency analysis of integrated dielectric lens antennas," *IEEE Trans. Antennas Propag.*, vol. 52, no. 3, pp. 840–847, Mar. 2004.
[17] D. Titz, F. Ferrero, and C. Luxey, "Development of a millimeter-wave measurement setup and dedicated techniques to characterize the matching and radiation performance of Probe-fed Antennas," *IEEE Antennas Propag. Mag.*, vol. 54, no. 4, pp. 188–203, Aug. 2012.
[18] D. Titz, F. Ferrero, P. Brachat, C. Luxey, and G. Jacquemod, "Efficiency measurement of probe-fed antennas operating at millimeter-wave frequencies," *IEEE Antennas Wireless Propag. Lett.*, vol. 11, pp. 1194–1197, Oct. 2012.
[19] *IEEE Standard for Safety Levels With Respect to Human Exposure to Radio Frequency Fields 3 kHz to 300 GHz*, IEEE Standard C95.1-2005, pp. 1–250, 2006.
[20] N. Chahat, C. Leduc, M. Zhadobov, and R. Sauleau, "Antennas and Interaction with the Body for Body Centric Wireless Communications at Millimeter Waves," in *Proc. Eur. Conf. Antennas Propag. (EuCAP)*, 2013, pp. 772–775.
[21] K. H. Chan, S. W. Leung, Y. L. Diao, Y. M. Siu, and K. T. Ng, "Analysis of millimeter wave radiation to human body using inhomogeneous multilayer skin model," in *Proc. Asia-Pac. Symp. Electromagn. Compat. (APEMC)*, 2012, pp. 721–724.
[22] A. R. Guraliuc, M. Zhadobov, G. Valerio, and R. Sauleau, "Enhancement of on-body propagation at 60 GHz using electro textiles," *IEEE Antennas Wireless Propag. Lett.*, vol. 13, pp. 603–606, Apr. 2014.
[23] M. Kouzai, A. Nishikata, T. Sakai, and S. Watanabe, "Characterization of 60 GHz millimeter-wave focusing beam for living-body exposure experiments," in *Proc. EMC'09*, 2009, pp. 309–312.
[24] M. Zhadobov *et al.*, "Evaluation of the potential biological effects of the 60-GHz millimeter waves upon human cells," *IEEE Trans. Antennas Propag.*, vol. 57, no. 10, pp. 2949–2956, Oct. 2009.
[25] M. Zhadobov, R. Sauleau, R. Augustine, C. Le Quément, Y. Le Dréan, and D. Thouroude, "Near-field dosimetry for in vitro exposure of human cells at 60 GHz," *Bioelectromagnetics*, vol. 33, no. 1, pp. 55–64, Jan. 2012.
[26] N. Chahat, M. Zhadobov, L. Le Coq, S. I. Alekseev, and R. Sauleau, "Characterization of the interactions between a 60-GHz antenna and the human body in an off-body scenario," *IEEE Trans. Antennas Propag.*, vol. 60, no. 12, pp. 5958–5965, Dec. 2012.

Q5 **Aimeric Bisognin** (S'xx) was born in Toulouse, France, in 1989. He received the Engineering degree in electronics from Polytech'Nice Sophia, Sophia Antipolis, France, in 2012, and the M.S. degree in telecommunications from EDSTIC, Sophia Antipolis, France, in 2012, and the Ph.D. degree in electronics engineering (with Hons.) from the University of Nice Sophia-Antipolis, France, in 2015.

During his Ph.D., he worked with the Electronique pour Objets Communicants (EpOC) Laboratory, STMicroelectronics, Crolles, France. He is currently a Postdoctoral Researcher with the EpOC Laboratory. He has authored or coauthored 8 publications in journals and 19 publications in international conferences. His research interests include millimeter-wave communications, especially in the field of the design and measurement of antenna in package, lens and reflector antennas for the 60, 80, and 120 GHz frequency bands.

Aykut Cihangir was born in Ankara, Turkey, in 1985. He received the Bachelor's degree in electrical and electronics engineering and the Master's degree Q6 from Middle East Technical University (METU), Ankara, Turkey, in 2010, and the Ph.D. degree from the University of Nice-Sophia Antipolis (UNSA), Nice, France, in 2007, 2010, and 2014, respectively.

Q7 From 2007 to 2011, he was with the Aerospace Industry as a Communication Systems Design Engineer in Unmanned Aerial Vehicle projects. Then, he was as a Postdoctoral Researcher with the EpOC team, UNSA. His research interests include electrically small antennas, matching networks, and mobile terminal antennas.

Cyril Luxey (SM'xx) was born in Nice, France, in 1971. He received the Master's degree (DEA) and the Ph.D. degree in electrical engineering (both with Hons.) from the University Nice-Sophia Antipolis, Nice, France, in 1996 and 1999, respectively.

During his thesis, he worked on printed leaky-wave antennas, quasi-optical mixers, and retrodirective transponders. From 2000 to 2002, he was with Alcatel, Mobile Phone Division, Colombes, France, where he was involved in the design and integration of internal antennas for commercial mobile phones. In 2003, he was an Associate Professor with the Polytechnic School, University Nice Sophia-Antipolis. Since 2009, he has been a Full Professor with the IUT Réseaux et Télécoms in Sophia-Antipolis, Valbonne, France. He is doing his research in the EpOC Laboratory as the Vice-Deputy of this laboratory. In October 2010, he was a Junior Member of the Institut Universitaire de France (IUF). Also, he collaborates with Berkeley Wireless Research Center, Berkeley, CA, USA, and Stanford University, Stanford, CA, USA, on mm-wave front-end transceivers at mm-wave frequencies. He also works on electrically small antennas, multiantenna systems for diversity, and MIMO techniques. He has authored or coauthored more than 250 papers in refereed journals, in international and national conferences and as book chapters. He has given more than 10 invited talks. His research interests include the design and measurement of millimeter-wave antennas, antennas-in-package, plastic lenses, and organic modules for 60, 120, and 240 GHz frequency bands.

Dr. Luxey is an Associate Editor for the IEEE ANTENNAS AND WIRELESS PROPAGATION LETTERS, a Regular Reviewer for several IEEE and IET journals and several European and US conferences in the field of microwave, microelectronics, and antennas. He has been the General Chair of the Loughborough Antennas and Propagation Conference 2011, the Award and Grant Chair of EuCAP 2012, and the Invited Paper CoChair of EuCAP 2013. He will be the TPC Chair of the EuCAP 2017 conference in Paris. He is also the Delegate of the French Research Ministry for the COST IC1102 action VISTA (Versatile, Integrated, and Signal-aware Technologies for Antennas) within the ICT Domain. He and his students received the H.W. Wheeler Award of the IEEE Antennas and Propagation Society for the best application paper of the year 2006. He was also the corecipient of the Jack Kilby Award 2013 of the ISSCC conference and the Best Paper Award of the EUCAP2007 conference, the Best Paper Award of the International Workshop on Antenna Technology (iWAT2009), the Best Paper Award at LAPC 2012, the Best Student Paper Award at LAPC 2013 (third place), the Best Paper Award of the ICEAA 2014 conference, and the Best Paper Award of the innovation contest of the iWEM 2014 conference (second place).

Gilles Jacquemod (M'xx) graduated from ICPI (CPE) Lyon, and received the M.Sc. degree (DEA) in microelectronics from Ecole Centrale Lyon, Écully, France, in 1986, the Ph.D. degree in integrated electronics from INSA Lyon, Lyon, France, in 1989.

From 1990 to 2000, he was with LEOM, Ecole Centrale Lyon, as an Associate Professor, on analog integrated circuit design and behavioral modeling of mixed domain systems. In 2000, he joined the LEAT Laboratory, Nice, France, the Ecole Polytechnique, Palaiseau, France, and Nice-Sophia Antipolis University, Nice, France, as a Full Professor. Since 2010, he has been with EpOC Research Team (URE UNS). He is the author and coauthor of more than 250 journal and conference papers, and holds 3 patents. His research interests include analog integrated circuit design and behavioral modeling of mixed domain systems. He is also involved in RF design applied to wireless communication.

Dr. Jacquemod is the Director of the CNFM PACA pole. He was the President of the CIM-PACA Design Platform.

Romain Pilard (M'xx) received the B.S. and M.S. degrees in electronics engineering from Polytech'Nantes, University of Nantes, Nantes, France, in 2006, and the Ph.D. degree in electrical engineering from Telecom Bretagne, Brest, France, in 2009.

Since 2010, he has been with the STMicroelectronics, Crolles, France, where he works on the development of integrated antennas and high-performance passive components in advanced bulk and SOI RF CMOS technologies. His research interests include millimeter-wave antenna design and packaging technology development.

Frédéric Gianesello (M'xx) received the B.S. and M.S. degrees in electronics engineering from the Institut National Polytechnique de Grenoble, Grenoble, France, in 2003 and the Ph.D. degree in electrical engineering from the Joseph Fourier University, Grenoble, France, in 2006.

He is currently working for STMicroelecetronics, Crolles, France, where he leads the team responsible for the development of electromagnetic devices (inductor, balun, transmission line, and antenna) integrated on advanced RF CMOS/BiMOS (down to 14 nm), silicon photonics, and advanced packaging technologies (3-D Integration, FOWLP, etc.). He has authored and coauthored more than 110 refereed journal and conference technical articles.

Dr. Gianesello has served on the TPC for the International SOI Conference from 2009 up to 2011 and he is currently serving on the TPC for the Loughborough Antennas and Propagation Conference (LAPC).

Jorge R. Costa (S'97–M'03–SM'09) was born in Lisbon, Portugal, in 1974. He received the Licenciado and Ph.D. degrees in electrical and computer engineering from the Instituto Superior Técnico (IST), Technical University of Lisbon, Lisbon, Portugal, in 1997 and 2002, respectively.

He is currently a Researcher with the Instituto de Telecomunicações, Lisbon, Portugal. He is also an Associate Professor with the Departamento de Ciências e Tecnologias da Informação, Instituto Universitário de Lisboa (ISCTE-IUL), Lisbon, Portugal. He is the coauthor of four patent applications and more than 100 contributions to peer reviewed journals and international conference proceedings. More than twenty of these papers have appeared in IEEE Journals. His research interests include lenses, reconfigurable antennas, MEMS switches, UWB, MIMO, and RFID antennas.

Prof. Costa is currently serving as an Associate Editor for the IEEE TRANSACTIONS ON ANTENNAS AND PROPAGATION and he was a Guest Editor of the Special Issue on "Antennas and Propagation at mm- and Sub mm-Waves," from the IEEE TRANSACTIONS ON ANTENNAS AND PROPAGATION, April 2013. He was the Co-Chair of the Technical Program Committee of the European Conference on Antennas and Propagation (EuCAP 2015) in Lisbon.

Carlos A. Fernandes (S'86–M'89–SM'08) received the Licenciado, M.Sc., and Ph.D. degrees in electrical and computer engineering from Instituto Superior Técnico (IST), Technical University of Lisbon, Lisbon, Portugal, in 1980, 1985, and 1990, respectively.

He joined IST in 1980, where he is currently a Full Professor with the Department of Electrical and Computer Engineering in the areas of microwaves, radio wave propagation and antennas. He is a Senior Researcher with the Instituto de Telecomunicações and member of the Board of Directors. He has coauthored a book, a book chapter, more than 150 technical papers in peer-reviewed international journals and conference proceedings and 7 patents in the areas of antennas and radiowave propagation modeling. His research interests include dielectric antennas for millimeter wave applications, antennas, and propagation modeling for personal communication systems, RFID and UWB antennas, artificial dielectrics, and metamaterials.

Dr. Fernandes was a Guest Editor of the Special Issue on "Antennas and Propagation at mm- and Sub mm-Waves," from the IEEE TRANSACTIONS ON ANTENNAS AND PROPAGATION, April 2013.

Eduardo B. Lima (S'14) received the Licenciado and M.Sc. degrees in electrical and computer engineering from the Instituto Superior Técnico (IST), Technical University of Lisbon, Lisbon, Portugal, in 2003 and 2008, respectively. He is currently working toward the Ph.D. degree at IST.

He is also currently a Researcher with the Instituto de Telecomunicações (IT), Lisbon, Portugal. Since 2004, he has been also responsible for development and maintenance of all measurement control systems at the RF laboratories. He is the coauthor of one patent application and 32 technical papers in international journals and conference proceedings in the area of antennas. One of which was awarded the CST University Publication Award 2010. His research interests include dielectric lens antennas, Fabry–Pérot cavity antennas, and transmit arrays.

Dr. Lima is currently serving as a Technical Reviewer for the IEEE TRANSACTIONS ON ANTENNAS AND PROPAGATION (TAP) and he also served as a TPC member in the EuCAP2015 conference.

Chinthana J. Panagamuwa (M'xx) received the Master of Engineering (M.Eng.) degree in electronic and electrical engineering and the Ph.D. degree in electronic and electrical engineering from Loughborough University, Loughborough, U.K., in 2000 and 2005, respectively.

Since 2007, he has been a Lecturer in Photonic Systems with the Wolfson School of Mechanical, Manufacturing, and Electrical Engineering, Loughborough University. His research interests include optically activated semiconductor switches for microwave circuits, devices and antennas. He also conducts research on specific absorption rates due to mobile communications devices and in-body antennas.

Since 2011, he is the Coordination Chair of the Loughborough Antennas and Propagation Conference series.

William G. Whittow (M'12–SM'12) received the B.Sc. degree in physics and the Ph.D. degree in computational electromagnetics from the University of Sheffield, Sheffield, U.K., in 2000 and 2004, respectively.

From 2004 to 2012, he was a Research Associate with the School of Electronic, Electrical and Systems Engineering, Loughborough University, Loughborough, U.K. He was a Lecturer in Electronic Materials Integration, University of Loughborough, in 2012 and he became a Senior Lecturer in May 2014. He has authored more than 150 peer-reviewed journal and conference papers in topics related to electromagnetic materials, synthetic dielectrics, wearable antennas, VHF antennas, specific absorption rate, FDTD, bioelectromagnetics, meta-materials, heterogeneous substrates, embroidered antennas, inkjet printing, electromagnetic compatibility, phantoms and Genetic Algorithms.

Dr. Whittow was the Coordinating Chair of the Loughborough Antennas and Propagation Conference (LAPC). He is an Associate Editor of *Electronics Letters*. He serves on the technical programme committees of several IEEE international conferences. He has been asked to give 6 invited conference presentations and a 4-day invited workshop on bioelectromagnetics.

QUERIES

Q1: Please provide postal code for all the affiliations.
Q2: Please provide author name and year of publication for Refs. [1]–[5], and [14].
Q3: Please provide page range for Ref. [11].
Q4: Please provide complete details for Ref. [15].
Q5: Please provide membership history (year) for authors "Aimeric Bisognin, Cyril Luxey, Gilles Jacquemod, Romain Pilard, Frédéric Gianesello, and Chinthana J. Panagamuwa."
Q6: Please provide field of study for Master's and Ph.D. degrees of author "Aykut Cihangir."
Q7: Please provide location for Aerospace Industry in the biography section.